General Disclaimer

One or more of the Following Statements may affect this Document

- This document has been reproduced from the best copy furnished by the organizational source. It is being released in the interest of making available as much information as possible.

- This document may contain data, which exceeds the sheet parameters. It was furnished in this condition by the organizational source and is the best copy available.

- This document may contain tone-on-tone or color graphs, charts and/or pictures, which have been reproduced in black and white.

- This document is paginated as submitted by the original source.

- Portions of this document are not fully legible due to the historical nature of some of the material. However, it is the best reproduction available from the original submission.

Produced by the NASA Center for Aerospace Information (CASI)

OLD DOMINION UNIVERSITY RESEARCH FOUNDATION

DEPARTMENT OF PHYSICS AND GEOPHYSICAL SCIENCES
SCHOOL OF SCIENCES AND HEALTH PROFESSIONS
OLD DOMINION UNIVERSITY
NORFOLK, VIRGINIA

Technical Report PGSTR-PH77-56

X-RAY EMISSION FROM HIGH TEMPERATURE PLASMAS

(NASA-CR-153290) X-RAY EMISSION FROM HIGH TEMPERATURE PLASMAS Final Report, 1 Jul. 1974 - 30 Jun. 1977 (Old Dominion Univ., Norfolk, Va.) 79 p HC A05/MF A01 CSCL 20I
N77-27920
Unclas
G3/75 36782

By

Wynford L. Harries

Final Report

Prepared for the
National Aeronautics and Space Administration
Langley Research Center
Hampton, Virginia 23665

Under
Research Grant NSG 1022
July 1, 1974 - June 30, 1977
Dr. Frank Hohl, Technical Monitor
Environmental and Space Sciences Division

July 1977

JUL 1977
RECEIVED
NASA STI FACILITY
INPUT BRANCH

DEPARTMENT OF PHYSICS AND GEOPHYSICAL SCIENCES
SCHOOL OF SCIENCES AND HEALTH PROFESSIONS
OLD DOMINION UNIVERSITY
NORFOLK, VIRGINIA

Technical Report PGSTR-PH77-56

X-RAY EMISSION FROM HIGH TEMPERATURE PLASMAS

By

Wynford L. Harries

Final Report

Prepared for the
National Aeronautics and Space Administration
Langley Research Foundation
Hampton, Virginia 23665

Under
Research Grant NSG 1022
July 1, 1974 - June 30, 1977
Dr. Frank Hohl, Technical Monitor
Environmental and Space Sciences Division

Submitted by the
Old Dominion University Research Foundation
Norfolk, Virginia 23508

July 1977

TABLE OF CONTENTS

	Page
1. INTRODUCTION	1
2. RESULTS AND DISCUSSION	4
2.1. Focus I	4
2.1.1. Trajectories of High Energy Electrons in a Plasma Focus	4
Introduction	4
Experimental Method and Results	5
Discussion	11
Conclusions	15
Acknowledgements	18
References	19
List of Figures	21
Figures	22
2.1.2. Detection of Ion Trajectories	28
2.1.3. Spatial Distribution of Neutron Emission	29
2.1.4. Space and Time Resolved Emission of Hard X-Rays from a Plasma Focus	30
References	36
List of Figures	37
Figures	38
2.1.5. Summary of the Work on Focus I	43
Trajectories of High Energy Electrons in a Plasma Focus	43
Space and Time Resolved Emission of X-Rays from a Plasma Focus	43
2.2. The Staged Plasma Focus	45
2.2.1. A Staged Plasma Focus--General Discussion	45
References	48
List of Figures	49
Figures	50
2.2.2. Formation of Current Sheets in a Staged Plasma Focus	53
Introduction	53
Apparatus	53

TABLE OF CONTENTS--concluded

		Page
	Diagnostics	54
	Results	54
	Conclusions	56
	References	57
	List of Figures	58
	Figures	59
2.2.3.	X-Ray and Neutron Emission from a Staged Plasma Focus	64
	Introduction	64
	Experimental Results	64
	Conclusions	66
	List of Figures	67
	Figures	68
2.2.4.	Summary of Work on the Staged Plasma Focus	72
	References	73
3.	PUBLICATIONS	74

X-RAY EMISSION FROM HIGH TEMPERATURE PLASMAS

By

Wynford L. Harries[1]

1. INTRODUCTION

The investigation was a continuation of contract NAS1-11707-23 which ran 1 July 1973 to 30 June 1974. It was then renamed NSG 1022 and this report covers the period 1 July 1974 to 30 June 1977.

The work was an experimental investigation carried out at NASA Langley Research Center using their facilities. The experiments were done on the Focus I, Focus II and Staged Plasma Focus devices in collaboration with J. H. Lee of Vanderbilt University working under NASA Grant NGR 43-002-031, and D. R. McFarland of NASA.

The purpose of the work was to investigate the physical processes occurring in Plasma Focus devices. These devices produce dense high temperature plasmas, which emit x-rays of hundreds of KeV energy and 10^9-10^{10} neutrons per pulse. The processes in the devices seem related to solar flare phenomena, and would also be of interest for controlled thermonuclear fusion applications. The high intensity, short duration bursts of x-rays and neutrons could also be possibly used for pumping nuclear lasers.

The specific objective was to investigate x-ray emission. The emission was closely related to the dynamics of the electrons and in particular the trajectories of the high energy electrons. Consequently a number of experiments were performed on Focus I to detect the direction and angular spread of the high energy electrons, by measuring the bremsstrahlung x-rays. The work on Focus I is described in Section 2 and details of these experiments are given in Section 2.1.1, "Trajectories of High Energy Electrons in a Plasma Focus."

---

[1] Professor of Physics and Geophysical Sciences, School of Sciences and Health Professions, Old Dominion University, Norfolk, Virginia 23508.

It became evident that accelerated beams of electrons existed, that could only have been formed by strong electric fields. These fields were directed away from the anode and would also accelerate the ions. The picture was found consistent with the converging beam model of neutron production, proposed previously by J. H. Lee. Therefore experiments were made to detect ions moving away from the anode and also to obtain the spatial distribution of neutron emission. The experiments were not successful, and brief details are given in Section 2.1.2, "Detection of Ion Trajectories," and Section 2.1.3, "Spatial Distribution of Neutron Emission."

In addition, a separate series of experiments was carried out on Focus I whose purpose was to observe the distribution in space and time of both visible light, and x-rays by streak and framing techniques. An electronic camera and an Imacon image intensifier were used. Observations on a faster time scale than any used hitherto might be important in determining the mechanisms of the focus. The method has worked successfully and details are given in Section 2.1.4, "Space and Time Resolved Emission of Hard X-Rays from a Plasma Focus." The work on Focus I is summarized in Section 2.1.5.

Several runs were made on Focus II, but severe difficulties were experienced, mainly due to: (a) the capacitor bank voltage of up to 50 KV (as compared to 20 KV for Focus I) caused corona and insulator breakdowns, (b) there was lack of synchronization of the spark gaps (initially there were 20, later reduced to 4). The period September through December 1974 was spent entirely carrying out engineering tests on the device, the details of which are not included here. No relevant experimental data was obtained.

The period November 1976 to the present was spent on the Staged Plasma Focus, a concept originated by J. H. Lee. The work on the Staged Focus is described in Section 2.2. In addition to x-ray emission, the scope of the work was broadened to investigate the behavior of interacting plasmas. A general discussion of the staged focus is given in Section 2.2.1. The experimental work devolved into two parts, first the current sheet formation, and second the x-ray and neutron emission. Details of the former are given in Section 2.2.2, "Formation of Current Sheets in a Staged Plasma Focus," and details of the latter are given in Section 2.2.3, "X-Ray and Neutron

Emission from a Staged Plasma Focus." The results on the Staged Focus are summarized in section 2.2.4.

The work on the Focus I machine has resulted in seven papers (refs. 1 to 4, 6 to 8) given at national and international meetings, which are shown in the bibliography on page 74. A manuscript (ref. 5) has been submitted for publication to Plasma Physics on "Trajectories of High Energy Electronics in a Plasma Focus," and another is in preparation on "Space and Time Resolved Emission of Hard X-Rays from a Plasma Focus." The work on the Staged Plasma Focus has resulted in three papers (refs. 9 to 11) to be presented at the IEEE International Conference on Plasma Science, May 23-25, 1977, and it is intended to write up the results for publication shortly.

The collaboration of Dr. J. H. Lee working under NASA grant NGR 43-002-031 and D. R. McFarland of NASA is gratefully acknowledged.

2. RESULTS AND DISCUSSION

2.1. Focus I

2.1.1. Trajectories of High Energy Electrons in a Plasma Focus

Introduction

The mechanism by which x rays of hundred of keV and neutrons are emitted from plasma focus devices (Mather, 1964) is not well understood. It was thought at first that the neutrons and x rays were emitted by thermal processes (Mather, 1965; Beckner, 1966, 1967), i.e., collisions of particles in isotropic Maxwellian distributions in the dueterum plasmas. The plasma densities were over 10^{19} cm^{-3} and the electron and ion temperatures were several kilovolts (Peacock et al., 1968). However, Beckner, Clothiaux, and Smith (1969) showed that the dominant x-ray emission was due to nonthermal high-energy electrons striking the anode and suggested that high electric fields existed. Bernstein et al. (1969) showed that the x-ray photon distribution did not appear to be due to electrons in a Maxwellian distribution. Instead, it obeyed a power law, and was proportional to $E^{-\gamma}$, where E is the photon energy and $\gamma = 2$ for $7 < E < 29$ keV. Lee, Leobbaka and Roos (1971) showed similar behavior occurred above 100 keV except that γ was about 4. Anisotropy in the intensity of x rays, with a reduced signal on axis, was also reported by Jalufka and Lee (1972). Maisonnier et al. (1975) have also suggested the plasma, in a Filippov-type device, was heated by an energetic electron beam.

Neutron production was also consistent with the concept that strong electric fields accelerate the ions to high velocities. A mechanism for the ion acceleration has been suggested by Bernstein (1970). The ion energy distribution was deduced from measured anisotropies of neutron energy and fluence by Lee et al. (1971, 1972).

However, several questions yet remained unanswered. First, what was the polarity of the fields? Recently, Newman and Petrosian (1975) claimed the field was directed toward the anode, and the electrons should be accelerated away from it. Second, could the polarity of the field change in time? Third, how did beams of accelerated particles cross the magnetic field configuration?

The purpose of this investigation is to determine the trajectories of the high-energy electrons in the focus by observing the Bremsstrahlung x-rays emitted, and to infer the electric field configuration from the trajectories. Section II describes the experimental method and results. The direction and angular spread of electron velocities are investigated, and new measurements of anisotropy of x-ray flux at different energies are reported. In section III measurements by other authors of ion and neutron anisotropy are discussed and shown to be consistent with our results.

Experimental Method and Results

A. Plasma-Focus Device

The plasma-focus device was a Mather type, and is reported elsewhere (Lee et al., 1971; Jalufka et al., 1972). It consisted of coaxial cylindrical electrodes, 23 cm long, with a cathode of 10 cm diameter, and an internal anode of 5 cm diameter, both of copper (Fig. 1). They were enclosed in an aluminum sphere of 2 mm wall thickness and 30 cm diameter. The filling gas was deuterium at about 5 Torr. The capacitor bank provided 25 kJ energy at 20 kV. During the "focus" state, the plasma was compressed into a volume $\approx 10^{-2}$ cm^3, with densities $\approx 10^{19}$ cm^{-3}, and electron temperatures of several kilovolts. Copious neutrons, $\approx 10^{10}$ per focus were produced as well as intense x rays of over 100 keV.

B. Spatial Distribution of X Rays

Pinhole camera techniques for x rays are well known (Beckner et al, 1969). In contrast to previous measurements, we have recorded x rays up to 100 keV energy, (values higher than the voltage of the capacitor bank and in a range where there were no copper lines.) The pinholes were in 2-cm thick lead and were tapered to a minimum diameter of 0.4 mm. Each camera had several pinholes and 1:1 images were formed on an image intensifier screen (Du Pont Chronex Lightning type), 15 cm behind the pinhole. Contact prints were recorded on Polaroid 3000 or 10,000 ASA film. X rays of energies above 1 keV were recorded through a 250 μm Beryllium window (Fig. 1, A), those above 15 keV through the 2 mm aluminum vacuum vessel as shown in Figure 1, B, and those above 20, 30 and 50 keV were recorded by using lead filters of 102, 254 and 762 μm thickness respectively, observing through the vessel. The filters were used simultaneously, and both single and multiple shots were recorded. The results are summarized in Fig. 2a and confirm the observations of Beckner et al (1969) that the soft x rays came from the plasma and the hard x rays from the anode surface. The new result here is that the hardest x rays were emitted from a small region of the surface, on the axis. Observations from C, (Fig. 1) confirmed that x rays above 30 keV were emitted from a radius of approximately 1 mm diamter.

The response of the intensifier screen-film combination was not determined, so pinhole images of the x rays were also recorded on two 9 x 9 rasters of type 400 thermoluminescent detectors (TLD) (Cameron et al, 1968). These were small cubes, 3 x 3 x 0.75 mm, and on exposure to x rays stored some of the energy in metastable states. On being heated in a commercial analyser, visible light was emitted proportional to the intensity of the x-ray dose. Their reliability is

discussed in Section D. X rays of energy greater than 15 keV and greater than 30 keV energy were recorded from 25 focuses (Fig. 2b). The readings were approximately proportional to x-ray intensity and confirmed Fig. 2a except that the TLD's showed that x rays of over 30 keV were emitted from the plasma approximately 0.5 cm above the anode. Both experiments showed the high energy x rays emanated from near the axis, consistent with a model based on an accelerated electron beam. A beam would also explain the erosion of the anode, which occurred on axis. The first few shots showed a just discernible depression of approximately 1 mm radius; after 100 focuses it was about 1 mm deep and several mm in diameter.

C. Direction of Electron Velocity Vectors

The angular spread of electron velocities was next estimated. The electron paths were determined from the x rays emitted, by using a "shadow" method. A hollow anode was constructed, with an aluminum cap forming its upper surface, which had a 5 mm diameter hole on axis (Fig. 3). The hole did not appear to affect the discharges, and x rays of over 30 keV were recorded by a pinhole camera at $\theta = 45^{\circ}$, outside the vacuum vessel. The aluminum cap was transparent to x rays of this energy so it was possible to record emission from the upper surface of the cap at A (Fig. 3b) and from the floor of the cavity at B, on the same film. The two outlines of the hole, indicated that the main body of > 30 keV electrons had traveled essentially in paths almost perpendicular to the anode surface with an angular spread of less than 10°. However, exposure to 20 focuses revealed the whole outline of the bottom of the cavity, suggesting lower energy electrons were traveling at large angles relative to the axis.

We next checked whether at any time there were some electrons traveling away from the anode. A pinhole camera monitoring region D of the vessel (Fig. 1) (for x rays > 15 keV observed through the vessel) showed no evidence of emission when the same film was exposed to over 20 focuses. An insulated aluminum plate was then positioned

above the anode (Fig. 4) and observed through a 250 μm beryllium window. The plate did not seem to affect the plasma parameters when its center was more than 3 cm above the anode, and focuses were still obtained even when it was only approximately 1 cm from the anode. However, at this position, the neutron emission was considerably reduced although x rays from the anode surface were still evident. The field of view of the camera encompassed the anode and plate and recorded emission from the plasma as in Fig. 2a, but none whatever was recorded from the plate at any position. X rays down to 1 keV from its lower surface would have been recorded if they had been present. The lack of emission suggests there were few high energy electrons streaming upwards at any time.

D. Angular Dependence of X-ray Emission

Angular dependence was measured using type 400 thermoluminescent detectors. There is a general impression that TLD's are unreliable for quantitative x-ray measurements. Wide variations in readings were found when the TLD's were inadequately shielded from reflected x rays. However, lead containers of 3 mm thickness (Fig. 1, E and F) designed so that the detector saw only the plasma, made the readings consistent; 18 detectors exposed simultaneously gave readings within ± 5%. Tests using lead filters to reduce x rays and boron filled polythylene to reduce neutron flux, showed the signals were approximately proportional to x ray and not neutron intensity.

The TLD readings, however, were dependent on the energy of the x rays. The fraction η of energy retained in the TLD was estimated by sending a collimated x-ray signal through two detectors in series. If the incident signal flux was I_0 and the signals from the first and second TLD were s_1 and s_2, respectively, then $s_1 = \eta I_0$ and $S_2 = \eta(1 - \eta)I_0$ or

$$\eta = 1 - s_2/s_1 \qquad (1)$$

A rough estimate of η vs energy E was made by using lead filters. The thickness of the filter essentially determined the lower energy limit for x ray transmission, while the upper energy limit was a rough estimate only, as the x ray distribution function versus E was not known. A value of 0.49 ± 0.05 was determined for x rays of $15 < E < 25$ keV, and a value of 0.15 ± 0.06 for the range of $30 < E < 50$ keV. (Backscatter of low-energy x rays into the rear TLD did not affect these estimates as the results were similar with a lead surface adjacent to the rear TLD, and with the surface removed 2 cm away, and shielded with aluminum, a good absorber.) The value of η will be used later in comparing emission of different energies.

Estimates of x-ray flux vs emission angle θ were made by placing the TLD's every 15° outside the vessel for $0 < \theta < \pi/2$ (Fig. 1,E). The anode and cathode intervened for $\pi/2 < \theta < \pi$ but readings at $\theta = \pi$ were obtained by placing detectors in a cavity 15 cm below the focus (Fig. 1,G). The detectors were protected by the cap H, 2 mm thick.

The cap was first made of copper, the usual anode material, so it was necessary to normalize readings at G through copper to those at E through aluminum. Therefore, detectors were also placed at F behind 2 mm copper. Separate runs were also taken with H of 2 mm aluminum; the discharge parameters seemed to be unaffected by changing H from copper to aluminum.

At each angle θ, energy analysis was performed by simultaneously using lead filters of thicknesses 0, 102, 203, 256, 508 and 762 μm. Three detectors recorded for each filter, except at G where there was only one per filter (insufficient space). Emission from over 20 focus shots was superimposed on the TLD's for each anode material. The upper limit to the number of shots was dictated by the amount of erosion of the cap, which was small in each instance.

Polar diagrams of intensity of x rays in the 15 keV range with an aluminum cap were obtained (Fig. 5a). The points at $\theta = \pi/2$ are due to the anode and cathode intercepting the x rays. The pattern confirms reduced emission at $\theta = 0^{\circ}$ (Jalufka et al, 1972). The extra point at $\theta = \pi$ suggests the pattern is a cardioid. However, the pattern for aluminum with a 762 μm filter, (energies > 50 keV) (Fig. 5b) is greatly different. The signals were reduced two orders of magnitude, but more important, a forward lobe $(\theta = \pi)$ about 50 times greater than the sideways or backward signal, was evident. The polar diagrams for intermediate energies were intermediate between a cardioid and a narrow lobe.

Similar results were obtained with copper. The 2 mm thick copper transmitted energies > 30 keV, and the two triangles (Fig. 5a) normalized to the signal at 45° suggest a slightly forward oriented lobe. X rays > 50 keV showed a pronounced lobe with a forward to back ratio of about 40 to 1. The pronounced anisotropy of the high energy x rays will be discussed in Section III.

E. Total X-ray Energy Emitted

The total x-ray energy per focus was estimated using TLD's which had been calibrated using a standard x-ray source. The estimate was in order of magnitude only, as the energy dependence of the emission from the plasma and the calibration source were different. The relative response to the TLD's to the 0.662 MeV x rays from the Cs 137 source was about 1/10 the response to x rays of 10 to 100 keV (Cameron et al, 1968). The average dose per focus on TLD's placed 15 cm away outside the vessel at $\theta = 45^{\circ}$, was approximately 4 mR. Assuming 1% transmission (averaged over energy) through 2 mm aluminum, the total energy per focus for x rays >15 keV was of order 10 mJ. The dose on a TLD measuring x rays > 50 keV at $\theta = 45^{\circ}$ was 50 times smaller than the dose at $\theta = \pi$. The total energy per focus for x rays

> 50 keV was estimated to be $\approx$ 1 mJ, after taking account of the anisotropy.

F. Time of Emission of X Rays

The purpose of this experiment was to see if the x rays from the plasma and from the anode surface were emitted at different times. A pinhole camera formed an image on an intensifying screen, and two light pipes were placed against the image, observing the dense focus region, and the anode surface region respectively. The light signals were monitored with two separate photomultipliers and displayed on an oscilloscope.

The light pipes used were polished aluminum tubes, as the commercially available fiberglass type became fluorescent from the x rays and neutrons. The intensifying screen had a rise time of a few ns, and a decay time of several ms. The x rays from the focus region were observed to occur 20 ns before those from the anode surface region. The latter signal continued to increase in amplitude for several hundred nanoseconds, indicating that x-ray emission persisted beyond the apparent focus lifetime of 200 ns. This long emission time was in agreement with the scintillation detector signal.

Discussion

In the dense focus, values of $n_e = 10^{19}$ cm^{-3}, and T_e and T_i of several keV are generally accepted. Assuming T_i and T_e = 3 keV, the electron and ion self collision times are estimated as 1 and 60 ns respectively. The duration of soft x-ray emission from the focused plasma, which for our purposes we shall regard as a containment time τ_c, is about 200 ns, so the electron velocity distribution should be Maxwellian in the focus. Here the Debye length is estimated as 10^{-5} cm, much less than the plasma dimension, so the focused plasma probably maintains

electrical neutrality. Indeed low-energy x rays corresponding to an electron temperature of a few keV are observed as in Fig. 2(a).

The rasters of Fig. 2(b) which were placed on the image plane of a pinhole camera were used to obtain the spatial distribution of the ratios of doses through two different filters. The ratios can yield T_e if a Maxwellian distribution is established by using the method of Elton and Anderson (1967). Unfortunately, the doses through the thicker filter corresponding to the dense focus region about 2 cm above the surface were too small to be measured, even after exposures to 25 focuses. Estimates of 5 to 10 keV electron temperature were obtained for the region about 0.5 cm above the anode, but it is doubtful that a Maxwellian distribution is applicable there. The ratios, however, give some measure of an average energy for the electrons. The ratios decrease on approaching the anode surface implying a higher average energy there than in the plasma. The region of highest energy is on axis on the anode surface. Very qualitative estimates of point by point intensity ratios taken from the intensifier screen-polaroid film combination confirm this result.

The observation of x rays of energies > 50 keV from the anode surface on axis, (Fig. 2 and Fig. 3b) implies electrons are traveling in a beam toward the anode. Therefore, strong electric fields exist between the dense focus and the anode, sufficient to accelerate electrons to energies of order 100 keV over a distance of order 1 cm. Fields of such magnitude would have caused all electrons over 200 eV to run away if $\eta_e = 10^{19}$ cm^{-3} (particle-particle collisions only are taken into account).

We consider next the effect of the magnetic field $B_\theta(r)$ created by the current through the plasma on the electron trajectories. The total current is about 1 MA at the instant of focus formation and should create an azimuthal magnetic

field of 100 T around the current column of radius $r_o = 1$ mm. Inside the current column $B_\theta(r) \propto r$; $r < r_o$, (assuming constant current density, which may not be true). During compression, the plasma and field are "frozen" together (the diffusion time through a distance r_o at $T_e = 3$ keV is 4×10^{-4} sec, much greater than τ_c). However, on axis, $B_\theta(0) = 0$ so a beam of particles can travel on or near the axis from the focus to the anode without deflection by the field.

The polar diagrams (Fig. 5) confirm the high energy x rays are caused by electrons with an anisotropic velocity distribution. The emission of Bremsstrahlung from a directed beam of electrons is well known, and the intensity $\Pi(\phi)$ per electron per unit solid angle per sec. is (see, for example, Leighton, 1959):

$$\Pi(\phi) = \frac{q^2 a^2 \sin^2 \phi}{16 \pi^2 \varepsilon_o c^3 (1 - \beta \cos \phi)^5} \qquad (2)$$

Here q is the charge of the electron, a magnitude of the acceleration, ε_o the dielectric constant of free space, $\beta = v/c$, v the electron velocity, c the velocity of light, and ϕ the angle of emission relative to the forward direction of the electron. The radiation patterns for different electron energies (Fig. 6a) show that as β increases, the radiation is predominantly forward. Then the intensity at $\theta = \pi - \phi$ would be the sum of patterns similar to Fig. 6a from electrons whose velocity vectors lie in a cone at any angle up to α relative to the axis of symmetry (Fig. 6(b)). The intensity versus θ for 20 keV would be a cardioid, (Fig. 5(a)) and for 100 keV would resemble a forward lobe, (Fig. 5(b)). The pattern for copper ($\approx$ 30 keV) would be intermediate, as observed.

Although the emission is thick target Bremsstrahlung, the argument is still consistent as the high-energy Bremsstrahlung is mostly due to first deflections. Comparison of Figs. 5(b) and 6(a) suggest values of $\beta \approx 0.5$ indicating electrons

of energy approaching 100 keV, consistent with the transmission data obtained with lead filters.

Very rough estimates of the total energy in the runaway current can be made. Our measurements show the total energy in x rays above 50 keV is of order 1 mJ. The runaway current is estimated assuming it consists of a monenergetic beam of electrons, all of energy $E = 50$ keV. The efficiency of energy conversion from such a beam into x rays is roughly

$$\alpha = 10^{-9} EZ \tag{3}$$

where Z is the atomic number of the target (Patou, 1970). Then α is 1.5×10^{-3} and hence the electron beam energy is of order 1J.

A beam of 50 keV electrons lasting for 100 ns and of 1J total energy corresponds to an average current of 200 A.

A theoretical estimate of the runaway current in a focus has been made by Hohl and Gary (1974). They assume that the beam has much higher current density than the surrounding plasma, and creates the magnetic field in its neighborhood. Then all particles within a gyroradius r_L of the axis (r_L is calculated from the field at the edge of the beam) contribute to the runaway current I_{run}:

$$I_{run} = 2\pi(mKT)^{1/2}/\mu_o e \tag{4}$$

where m is the mass, e the charge, T the temperature of the particle, and μ_o the permeability of free space. For electrons with $kT_e = 3$ keV, $I_{run} = 600$A agreeing in order with our values. The theory yields a beam radius of 1 μm. The experiments (hard x-ray emission, (Fig. 2(a), and the erosion) indicate a beam diameter of approximately 1 mm at the anode surface. However, there could have been spreading of the beam between the focus region and the surface of the anode.

Estimates of beam currents in a focus device are reported by Maissonier et al (1975) which are several orders of magnitude higher than ours. However, the experiments were performed in a Filippov type device with a 40 kV, 74 kJ capacitor bank. Any comparison with their results is difficult because of very different parameters.

The plasma sheath is probably formed just after maximum compression because the plasma x rays appear slightly before the x rays from the anode. This picture is consistent with computer simulations of Hohl et al, (1974).

The electric field should also accelerate ions away from the anode. Evidence of erosion was clearly visible on the inner surface of the vacuum vessel at $\theta = 0^{\circ}$. Recently Gullickson (1975) has shown that the flux of energetic ions from a Mather device showed a very sharp peak at $\theta = 0^{\circ}$.

The production of neutrons is also consistent with a beam of ions accelerated to energies of order 100 keV, and converging on the dense plasma. This mechanism has been proposed previously by one of us (Lee et al, 1971) as the converging beam model to explain the observed anisotropy of the neutron flux of the plasma focus.

Conclusions

Spatial resolution of the x-ray emission from a plasma focus confirms that the low-energy x rays are emitted from the plasma and the high-energy (> 50 keV) x rays are emitted from the anode surface. In addition, new evidence is presented that the highest energy x rays come from a small region (diameter $\approx$ 1 mm) on axis as shown by an intensifier screen-polaroid sensor, by TLD rasters, and from anode erosion.

The low-energy emission is consistent with a thermal plasma of a few keV energy. The high-energy emission is consistent with an accelerated beam of electrons with energies of order 100 keV. The electron beam reaches the anode 20 ns after the dense plasma formation.

The existence of a directed beam of this energy implies a sheath region of very high fields between the dense focus and the anode. The presence of the sheath is assumed in this paper, and the mechanism by which it is created is not discussed.

The direction of the electron beam is essentially perpendicular to the anode, as shown by the "shadow" experiment. There does not seem to be any streaming away from the anode at any time as shown by lack of emission from the underside of the plate. The electrons gain energy on approaching the anode as shown by both the TLD raster and the intensifier screen-polaroid film experiments.

The plasma conditions are consistent with a "runaway" electron beam. The magnetic field configuration would have allowed the passage of the beam from the focus to the anode, only near the axis, as observed.

The energy and current in the beam are roughly estimated from the x-ray emission. The results are very approximate but show the beam energy for electrons over 50 keV is of order 1J and the current of order 200 A. A theoretical estimate yields 600 A - agreeing in order. Polar diagrams of x-ray intensity show that low-energy emission is approximately isotropic. However, there is marked anisotropy in x rays of energies over 50 keV, which show a lobe in the direction of the anode with a forward-to-back ratio of 50 to 1. The lobe is consistent with a relativistic beam of electrons of energies of order 100 keV directed toward the anode.

The above results show that the electric fields are directed away from the anode - a conclusion which contradicts the postulate of Newman and Petrosian (1975).

A field directed away from the anode would be consistent with the anistropy of ion flux, measured by Gullickson (1975), and also consistent with the converging beam model of neutron production (Lee et al., 1971).

Acknowledgements

The authors would like to thank Dr. Frank Hohl for his interest and support, and to both he and Dr. S. Peter Gary for valuable discussions. The work was carried out at the National Aeronautics and Space Administration Langley Research Center, and supported in part under grants NAS1-11707-23, NAS1-1022, and NGR 43-002-034.

References

Beckner, E. H., Clothiaux, E. J., and Smith, D. R., Phys. Fluids 12, 253 (1969).

Beckner, E. H., J. App. Phys. 37, 4944 (1966); Rev. Sci. Instr. 38, 507 (1967).

Bernstein, M. J., Meskan, D. A., and Van Paasen, H. L. L., Air Force Report No. SAMSO-TR-69-304 of September 1969.

Bernstein, M. J., Phys. Fluids 13, 2858 (1970).

Cameron, J. R., Suntharalingam, N., and Keeney, G. M., "Thermoluminescent Dosimetry" (Wisconsin Press)(1968).

Elton, R. C., and Anderson, A. D., Applied Optics 6, 2071 (1967).

Gullickson, R. H., "Measurement of the Distribution of Very Energetic Ions in the Plasma Focus Device," UCRL-76831 (1975).

Hohl, F. and Gary, S. P., NASA Technical Note TN-D7707, November 1974.

Hohl, F. and Gary, S. P., Phys. Fluids 20, 683 (1977).

Jalufka, N. W. and Lee, J. H., Phys. Fluids 15, 1954 (1972).

Lee, J. H., Shomo, L. P., Williams, M. D., and Hermansdorfer, H., Phys. Fluids 14, 2217 (1971).

Lee, J. H., Leobbaka, D. S., and Roos, C. E., Plasma Physics 13, 347 (1971).

Lee, J. H., Shomo, L. P., and Kim, K. H., Phys. Fluids 15, 2433 (1972).

Leighton, R. B., "Principles of Modern Physics," McGraw-Hill, 1959, p. 413.

Maissonier, C., Gourlan, C., Luzzi, G., Papagno, L., Pecorella, F., Rager, J. P., Robouch, B. V., and Samuelli, M., IV Conference on Plasma Physics and Controlled Nuclear Fusion Research, Madison, 1971, IAEA Vienna, Vol. 1, p. 523.

Maissonier, C., Pecorella, F., Rager, J. P., Samuelli, M., Strangio, C., and Messina, A., Comparative Studies of Plasma Focus Devices, IAEA-33/E6-2, Fifth Conference on Plasma Physics and Controlled Nuclear Fusion Research (Tokyo, Japan), November 1975.

Mather, J. W., Phys. Fluids Suppl. 7, S28 (1964).

Mather, J. W., Phys. Fluids 8, 366 (1965).

Newman, C. E. and Petrosian, V., Phys. Fluids 18, 547 (1975).

Patou, C., Journal de Physique, 31, 334 (1970).

Peacock, N. J., Wilcock, P. D., Speer, R. J., and Morgan, P. D., Third Conference on Plasma Physics and Controlled Nuclear Fusion Research, Novosibirsk, U.S.S.R., 1-7 August 1968.

Van Paassen, H. L. L., Vandre, R. H., and White, R. S., Phys. Fluids 13, 2606 (1970).

List of Figures

Figure 1. Experimental Arrangement. Pinhole cameras observed the plasma through 250μm beryllium window, A, and through the aluminum vessel at B and C. Camera at D observed the vessel on axis. The thermo-luminescent detectors, E, were placed outside the vessel at different θ, and also inside the vacuum system, behind a copper shield at F, and in the hollow anode at G. The anode cap H was interchangeable.

Figure 2. Summary of pinhole results: (a) with intensifier screen-polaroid film combination, (b) readings proportional to x-ray intensity from TLD rasters.

Figure 3. Method of determining high energy electron trajectories from x-rays emitted: (a) structure of anode, (b) view observed by pinhole camera; x-rays are emitted from surfaces A and B, showing the electron trajectories are almost perpendicular to the anode surface.

Figure 4. Arrangement for detecting high energy electrons traveling away from the anode. The aluminum plate was supported by an insulator from above. No x-ray emission from its lower surface was evident.

Figure 5. Polar diagrams of x-ray intensity: (a) medium energy x-rays; ⊙ aluminum cap corresponding to > 15 keV, △ copper cap corresponding to > 30 keV, (b) x-rays > 50 keV, aluminum cap. The scale is arbitrary.

Figure 6. (a) Radiation pattern from a single electron; (b) electron trajectories and electric field configuration.

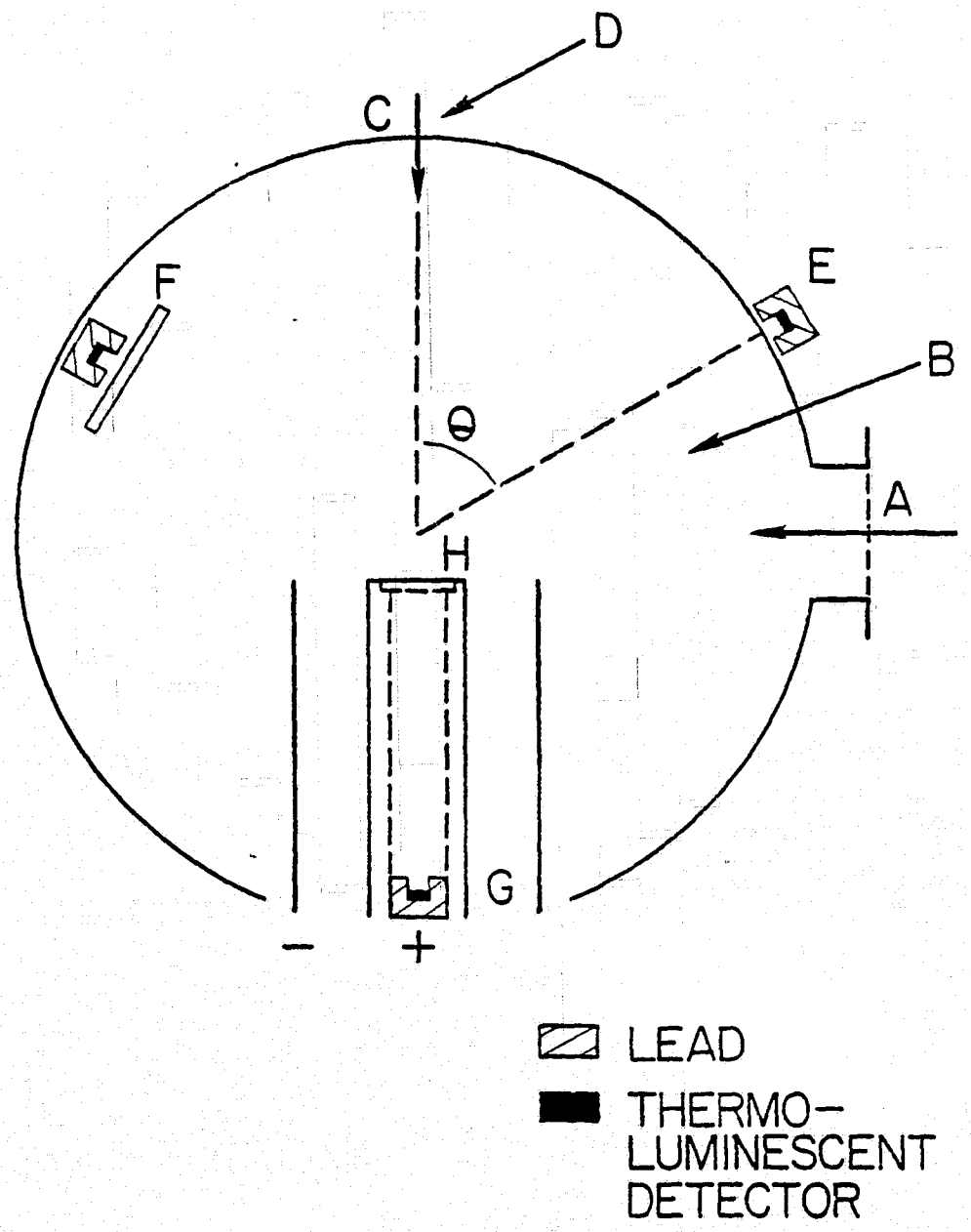

Figure 1. Experimental Arrangement. Pinhole cameras observed the plasma through 250μm beryllium window, A, and through the aluminum vessel at B and C. Camera at D observed the vessel on axis. The thermoluminescent detectors, E, were placed outside the vessel at different θ, and also inside the vacuum system, behind a copper shield at F, and in the hollow anode at G. The anode cap H was interchangeable.

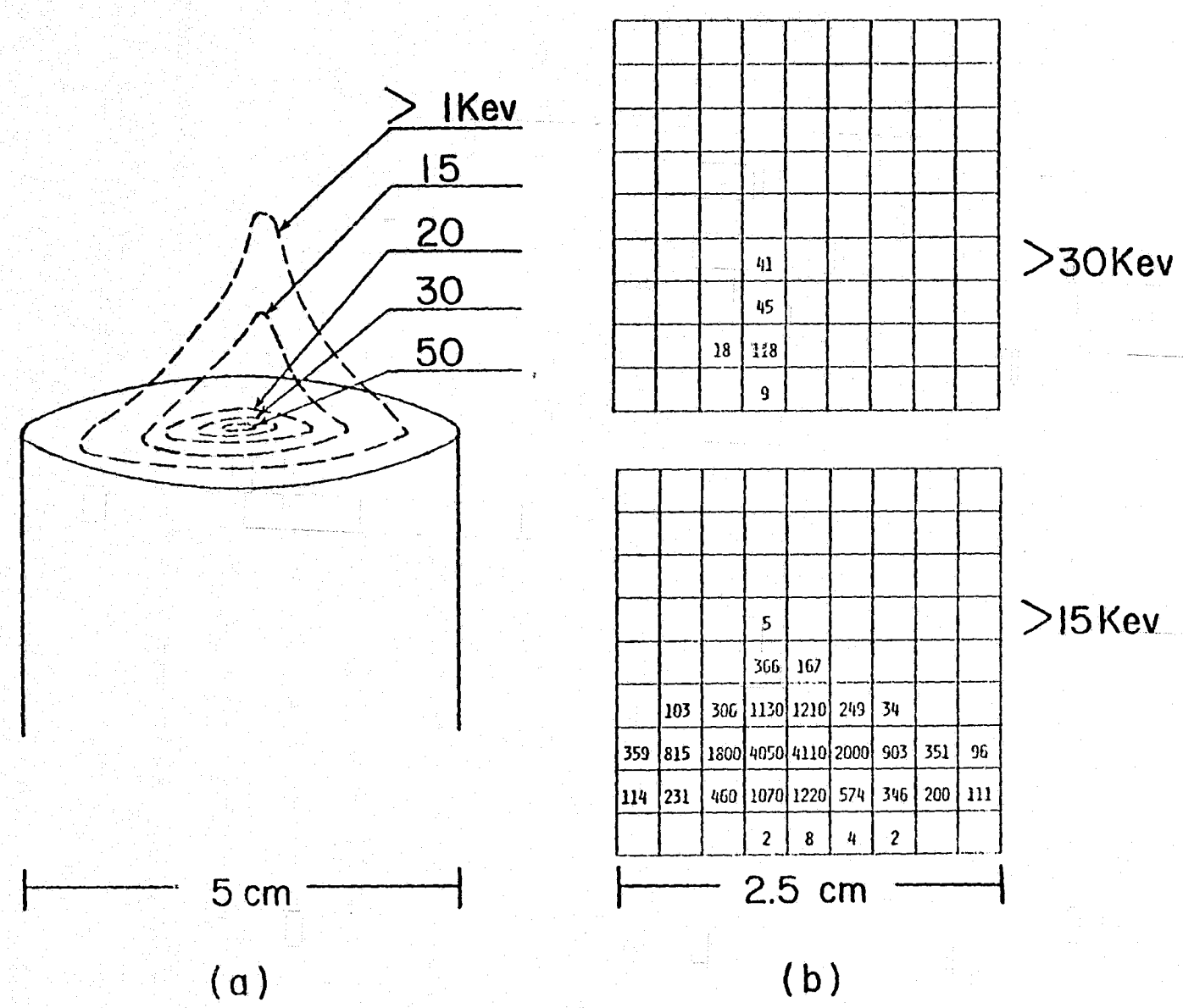

Figure 2. Summary of pinhole results: (a) with intensifier screen-polaroid film combination, (b) readings proportional to x-ray intensity from TLD rasters.

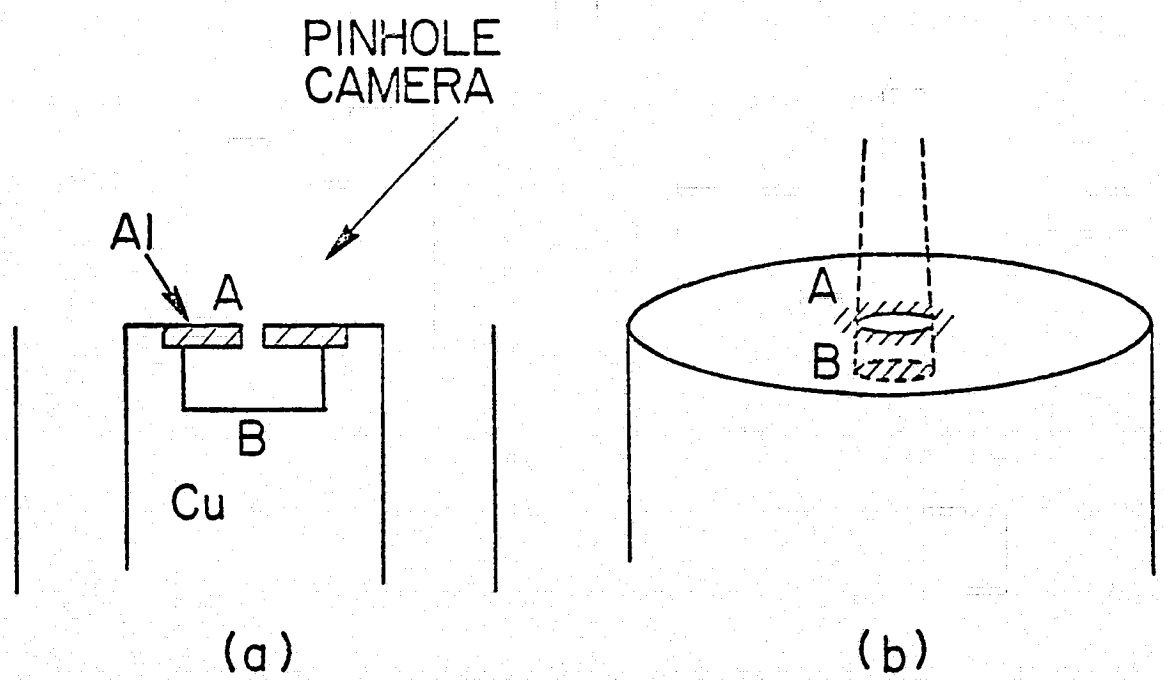

Figure 3. Method of determining high energy electron trajectories from x-rays emitted: (a) structure of anode, (b) view observed by pinhole camera; x-rays are emitted from surfaces A and B, showing the electron trajectories are almost perpendicular to the anode surface.

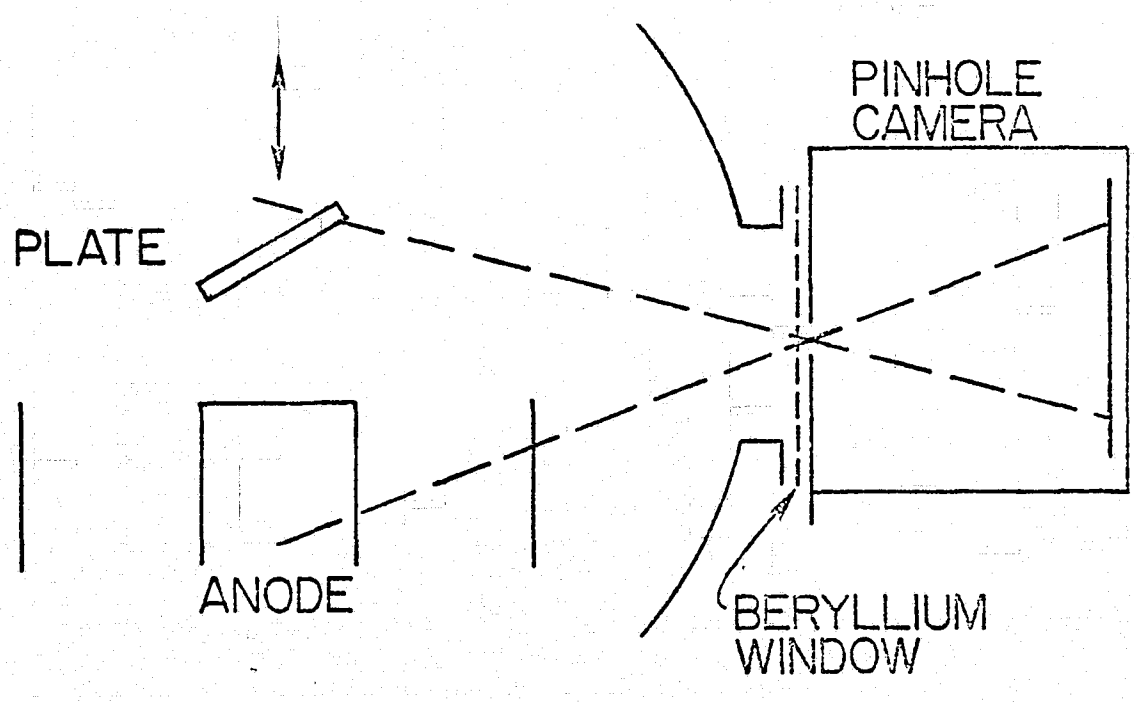

Figure 4. Arrangement for detecting high energy electrons traveling away from the anode. The aluminum plate was supported by an insulator from above. No x-ray emission from its lower surface was evident.

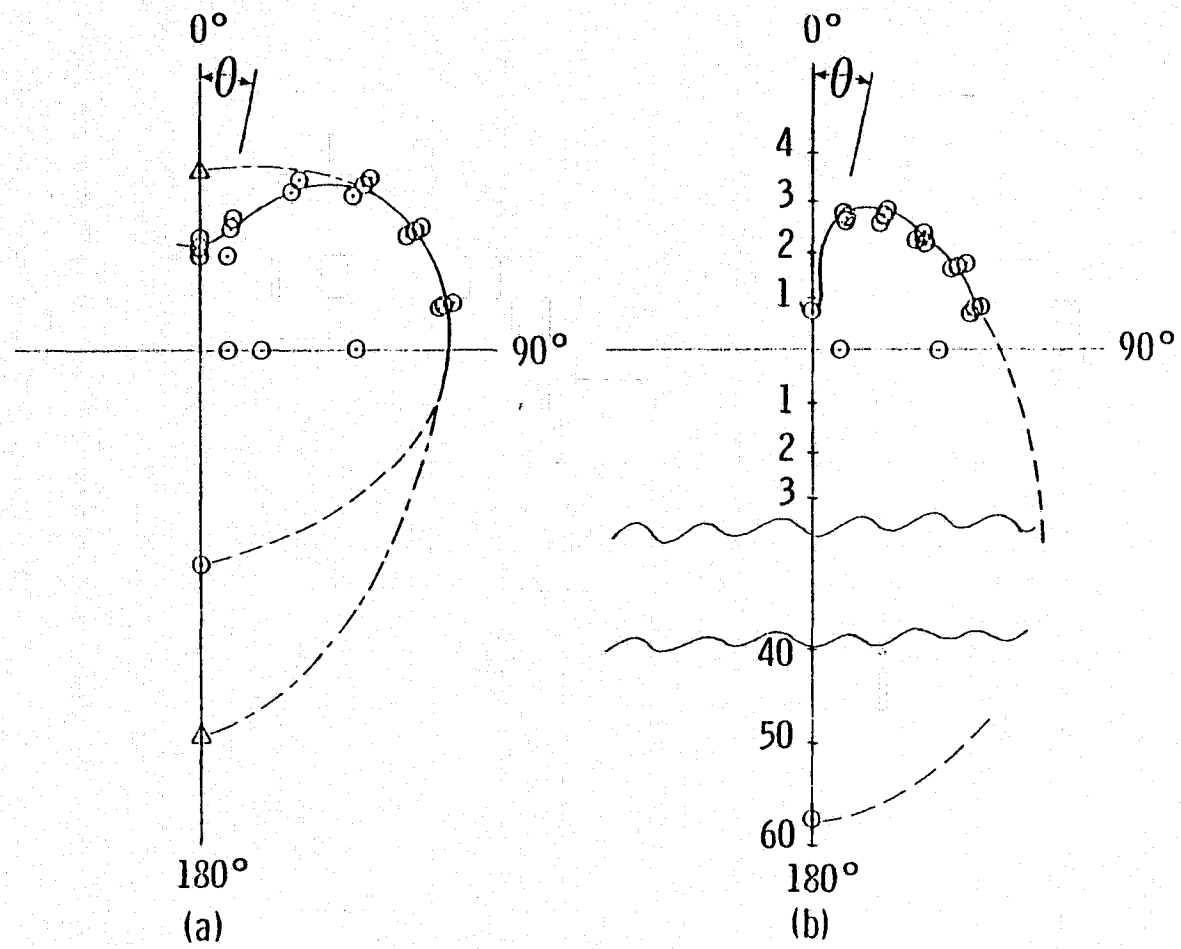

Figure 5. Polar diagrams of x-ray intensity: (a) medium energy x-rays; ⊙ aluminum cap corresponding to > 15 keV, △ copper cap corresponding to > 30 keV, (b) x-rays > 50 keV, aluminum cap. The scale is arbitrary.

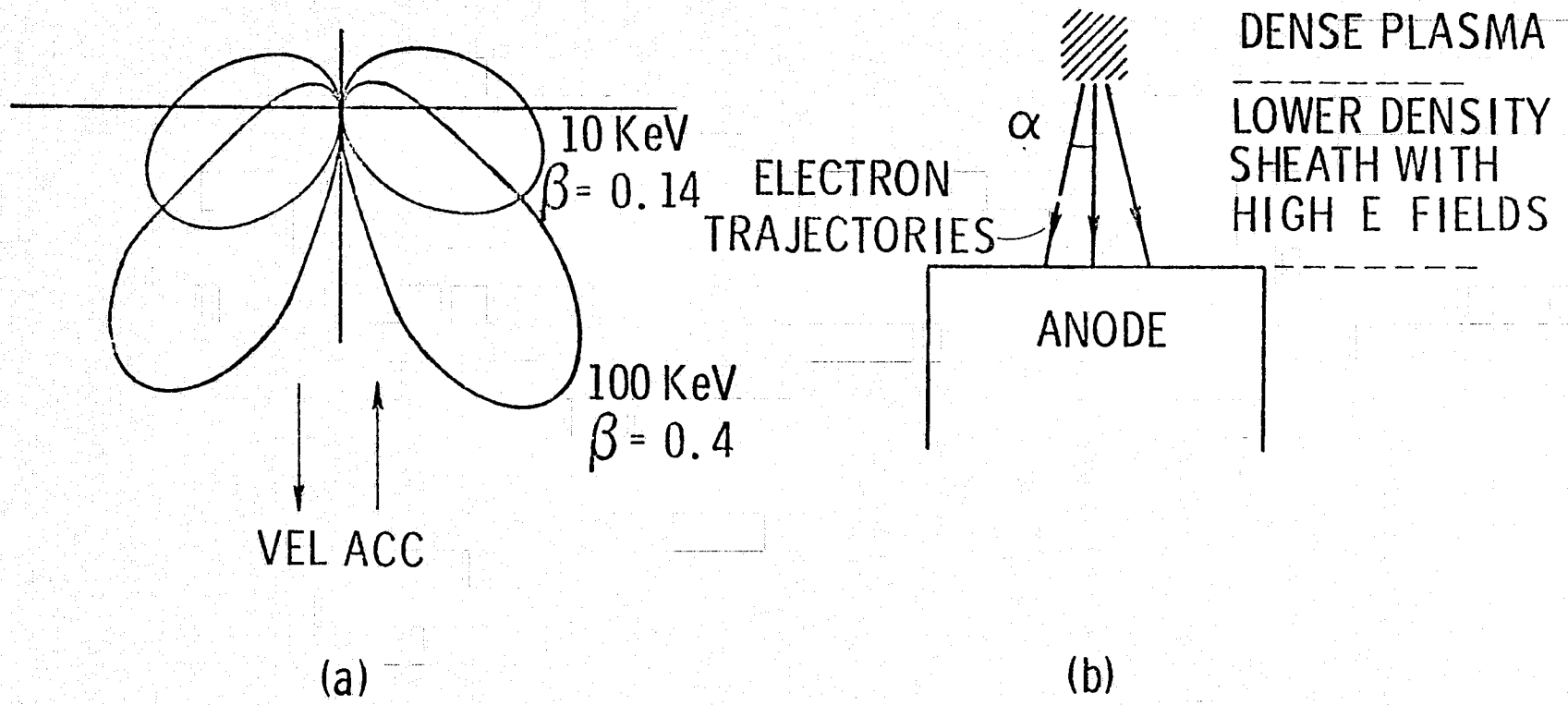

Figure 6. (a) Radiation pattern from a single electron; (b) electron trajectories and electric field configuration.

2.1.2. Detection of Ion Trajectories

The purpose of this experiment was to detect ions moving away from the anode, and if possible estimate their velocities.

Several methods were tried but all were unsuccessful. First, an aluminum plate insulated from the vessel was placed on axis and connected by cable to a 50 Ω resistor across the input of an oscilloscope. The ion flux should generate a positive voltage signal on the plate. Unfortunately, the signal was buried in noise, although double shielding was used. A Teflon cylinder 15 cm long was then placed between the vessel and the plate, to remove the plate from the region of strong electrical noise, but any signal was still undetectable, even using differential amplifier methods.

Next, several Rogowski coils were constructed that should have detected any ion current traveling to the plate through the Teflon cylinder. The coils were connected to differential amplifiers and made symmetrical so that the noise picked up would cancel. The system was double shielded, but the signals could still not be detected. In addition, a balanced, ferrite core transformer feeding a differential amplifier was constructed with a flat response up to 20 Mc, but this also failed to detect any signal.

The failure to detect any signal may possibly be caused by the space charge of the ions being cancelled out by electrons, dragged with them.

2.1.3. Spatial Distribution of Neutron Emission

An attempt was made to determine the spatial distribution of neutrons by using a collimator similar in cross section to the one shown in figure 1 of section 2.1.4. It was made of boron filled polyethylene, and had a two-dimensional array of 1 mm diameter holes spaced 2.54 mm apart. The collimator was 15 cm thick and observed neutrons from the focus through the 2 mm aluminum vacuum vessel. A 254 μm lead shield reduced the x-ray flux. The neutrons were detected by two methods: (a) by rods of NE102 scintillator placed in the holes and in contact with 3000ASA film, and (b) by using a 4 × 24 raster of Type 600 thermoluminescent detectors which should detect neutrons. After a run of 50 focuses no definite pattern was evident on the film. The scintillator rods were then removed and the TLD's positioned. Previous estimates showed that about 500 focuses should give reasonable signals, and a total of 532 were superimposed over a period of weeks. However, no firm conclusions could be drawn from the experiment.

2.1.4. Space and Time Resolved Emission of Hard X-Rays from a Plasma Focus

The problem of recording x-ray emission from a Plasma Focus devices versus space and time is difficult because the time scale is of order 100 ns. One method is to convert the x-ray image into a visible one, and use electronic cameras. Bernstein and Hai (1970) used such a technique but in order to enhance the bremsstrahlung emission from the focus, they introduced 8 percent of a high Z gas--argon. The results indicated that the regions of emission of visible light, and soft x-ray radiation, were more or less coincident, and that soft x-rays were emitted from the dense focus region and from near the anode surface almost simultaneously. This would be in accord with a general belief that x-ray pinhole cameras record emission from the focused plasma during the 100 ns focus duration.

Recently Rager (1975) has obtained framing pictures with an x-ray image intensifier (microchannel electron multiplier) gated at 10 ns, and showed well-defined images of the soft x-ray emitting regions. However, due to the characteristics of the detector, the hard x-ray ranges were not observed.

It is the purpose of this note to report the behavior of x-ray emission from focused plasmas using an image converter camera in the streak and framing modes. The above results have been extended by using a very high gain image intensifier which enabled much weaker hard x-ray emission (>20 KeV) to be recorded. Thus, the use of an admixture of higher atomic number into the deuterium was avoided, and the role of the vapor from the anode surface could now be discerned. In addition the time behavior of x-rays of different energies was also recorded for comparison.

The plasma-focus device used was a Mather type and has been described elsewhere (Lee et al., 1971; Jalufka et al., 1972). It consisted of a cathode of 10 cm diameter and an anode of 5 cm in diameter, both 23 cm long. They were enclosed in an aluminum sphere of 2 mm wall thickness and 30 cm diameter (fig. 1). The filling gas was deuterium at about 5 torr. The capacitor bank provided 25-kJ energy at 20 kV.

A lead collimator with a single vertical line of holes 1 mm diameter and 2.54 mm apart was placed opposite window A (fig. 1). The collimator was 15 cm long and placed adjacent to the window, which in turn was 15 cm from the focus; thus, a resolution approaching 1 mm was obtainable.

Both visible light and x-rays were recorded with the same collimator for comparison. For visible light, window A was quartz and the image plane B, ground glass. Crossed polaroid filters were used to reduce the visible intensity. For x-rays, window A was beryllium, 250 μm thick which passed x-rays >1 KeV. Detector B then converted the x-ray energy into visible light.

The material first used for the converter was NE102 plastic scintillator because its rise and decay times were a few nanoseconds. Various thicknesses were tried, and eventually thin rods 7.5 cm long were fitted into holes. but even they failed to give sufficient light intensity. The NE102 was therefore abandoned, and instead a DuPont Chronex Image Intensifying Screen was used. It had a rise time of a few ns and a decay time of about a microsecond. Fortunately, its sensitivity was sufficient so that lead filters could be used for energy analysis.

The electronic image converter camera was a TRW 500, and further sensitivity was obtained by placing an Imacon image intensifier with a variable gain of up to 1000 in series with it; thus, a system gain of 500,000 was possible in principle. The output was recorded on Polaroid film of 10,000 ASA. In practice, gains of less than the maximum were used as otherwise the film became fogged. The camera and intensifier were about 2 m from the plasma focus and were completely enclosed in a grounded shield. All signal cables were double shielded.

The streak pictures were compared with oscilloscope traces of x-ray and neutron emission monitored with a scintillator-photo-multiplier combination (fig. 2). The upper trace (a) shows medium energy x-rays of >15 KeV, recorded on a 2 mm slab of NE102 observing through the aluminum vessel. It can be seen that the emission continued for several hundreds of nanoseconds. The lower trace shows x-rays of >120 KeV and neutrons, recorded through 2 mm of lead on a 7.5 cm thick slab of NE102. The slab was

3 m away from the focus; thus, the neutrons were separated from the x-rays by 160 ns time of flight. The duration of the signals implies the focus was over in about 100 ns.

Figure 2(b) is a (low gain) streak photo of visible light on the same time scale. The actual focus is the plume on the left. After the focus was over, the region of visible light emission seemed to move away from the anode surface at a velocity of about 1 cm per μs. Figure 2(c) shows a streak picture of x-rays >1 KeV. It proved impossible to record x-rays emitted during the focus but again the emission started near the anode surface and the region of emission moved away from the anode in time. The dark band was due to the camera. Figure 2(d) is a streak photo of x-rays recorded through a filter of 100 μm of lead in addition to the beryllium window. These x-rays were >25 KeV, an energy higher than the capacitor bank. The emission from near the anode surface was consistent with time integrated pinhole pictures of x-rays >25 KeV.

The next experiment recorded the intensity of x-rays of different energies (without space resolution) on the same film as a streak photograph. X-rays of >1 KeV coming through the beryllium window alone were recorded on an x-ray intensifying screen observed by a light pipe (fig. 3(a)). A lucite cone acting as a scintillator, placed outside the vacuum vessel and attached to a light pipe recorded x-rays >20 KeV. A similar cone observing through an additional 750 μm of lead recorded x-rays >50 KeV. The ends of the light pipes were placed on the same plane as the collimator intensifying screen and their signals recorded on the streak photograph. In figure 3(b), the upper trace is a streak picture of x-rays >1 KeV similar in figure 2(c), and the three lower traces record intensity versus time for different energies. The sensitivities of the three detectors were different so it is difficult to compare the intensities of one trace with another. However, their temporal behaviors can be obtained: the low energy x-rays were emitted for a much longer period of time than the medium and hard x-rays, and the times of maximum intensity for the latter occurred several hundred ns after the focus was over.

Figure 4 shows a streak photograph of x-rays >1 KeV on a scale of 750 ns with a resolution of about 10 ns. The signals corresponding to x-rays of different energies are also shown. The dark bands were again due to the camera. For this particular shot there seems to be a time when the region of high emission was moving away from the anode surface at a velocity of order

10^5 m/s. Also shown is a time-integrated pinhole picture of x-rays >1 KeV taken through the window on the opposite side of the vessel. The streak camera observed only the central region of the pinhole image, and the vertical scales of the pinhole and streak pictures are the same. The streak camera results suggest that the pinhole image was formed from the anode surface upwards. Thus the image of the plasma above the anode surface may have been recorded several hundreds of nanoseconds after the focus occurred.

Pinhole images of the x-rays were also recorded in the framing mode. The lead collimator in figure 1 was replaced by a lead pinhole camera with a pinhole of 0.5 mm diameter, and the same image intensifier screen was used. The timing of the frames relative to the focus is shown in figure 5(a) where the top trace records the medium energy x-rays versus time, and the lower trace the x-rays >120 KeV and neutrons as previously. Figure 5(b) shows framing images of 20 ns duration taken 500 ns apart. The two vertical bands are due to the camera. The framing pictures are typical and confirm that the x-rays recorded from the region above the electrode appeared well after the focus was over.

The x-rays recorded here appeared to be mainly from copper vapor evaporated from the anode surface. The depression in the anode on axis after some tens of discharges supported this view. The small diameter of the depression (≈ 1 mm) strongly implied it was caused by a beam of electrons on axis. Again, pinhole pictures of x-rays >50 KeV had showed emission from the anode surface near the axis, suggesting a localized beam (Harries et al., 1977). The volume of copper vaporized per discharge was estimated at 3×10^{-5} cm^3 so the average copper density would be roughly 10^{17} per cc (assuming a volume of order 10 cc) or of order the density of deuterium.

The emission coefficient for bremsstrahlung is proportional to $n_e n_i Z_{eff}^2$ where n_e is the electron density, n_i the density of copper ion, and Z_{eff} the ion charge and >>1 for copper.

The velocity of the edge of the emission region of 10^4 to 10^5 m/s corresponds to copper atoms at energies of >10 KeV. Such high velocities could only have been obtained from an intense electron beam.

The first question that arises is why do the time-integrated pinhole pictures show a cone with its vertex at the plasma focus? The emission depends critically on the average electron energy, and we believe this was greatest within a narrow beam on axis, which accounts for the narrow tip of the emission region. Between the tip and anode surface the electrons from the beam were diverging sideways, especially by Coulomb collisions with copper ions (cross section $\propto Z^2_{eff}$), resulting in the conical shape.

The second question is why is there a time lag of hundreds of ns before x-ray emission occurred from the region above the electrode? The time lag was the travel time of the copper vapor, but the electron beam must have been maintained for this period.

The third question is, how can the electric field driving the beam exist for this duration? The electric field here was due to annihilation of magnetic energy from the azimuthal field surrounding the focus. Flux annihilation did not cease with the formation of the focus; the dense hot plasma tended to exclude the magnetic field at the point. Also, measurements showed that the plasma current dropped to only about one third of its value during the focus. The remaining magnetic field then diffused into the plasma, but the diffusion time was estimated to be several 100 ns (we assume a diffusion distance $\approx$ 1 mm and $T_e \approx 3$ KeV , although the concept of temperature cannot be applied to an electron beam).

In conclusion the recorded bremsstrahlung emission was that from a metallic plasma of copper released from the anode surface by bombardment from an intense electron beam. The intensity of emission was determined by the density of copper as well as the density of energy of the electron beam. The main emission recorded occurred several 100 ns after the focus was over, which implies that the electric fields driving the beam existed for this duration. The fields were created by annihilation of magnetic flux, and a rough estimate of the diffusion time of the magnetic flux into the dense plasma suggests that the flux continued to be annihilated for a time much longer than the focus duration.

Lastly, time-integrated pinhole pictures of soft x-rays should be treated with caution, as they need not necessarily represent conditions during the formation of the plasma focus.

This work was supported by NASA grants NSG 1022 and NGR 43-002-031.

References

Bernstein, M. J. and Hai, F., Rev. Sci. Instrum. 41, 1843 (1970).

Harries, W. L., Lee, J. H., and McFarland, D. R., Bull. Am. Phys. Soc. 22, 499 (1977).

Jalufka, N. W. and Lee, J. H., Phys. Fluids 15, 1594 (1972).

Lee, J. H., Leobbaka, D. S., and Roos, C. E., Plasma Physics 13, 347 (1972).

Rager, J. P., Third Topical Conference on High Beta Plasmas, 9-12 September 1975, Culham, England.

List of Figures

Figure 1. Method of taking streak photographs.

Figure 2. Streak photographs of visible light and x-rays.

Figure 3. Streak photographs of x-rays of different energies.

Figure 4. Comparison of streak and pinhole photographs of x-rays >1 KeV.

Figure 5. Framing pictures of x-rays >1 KeV.

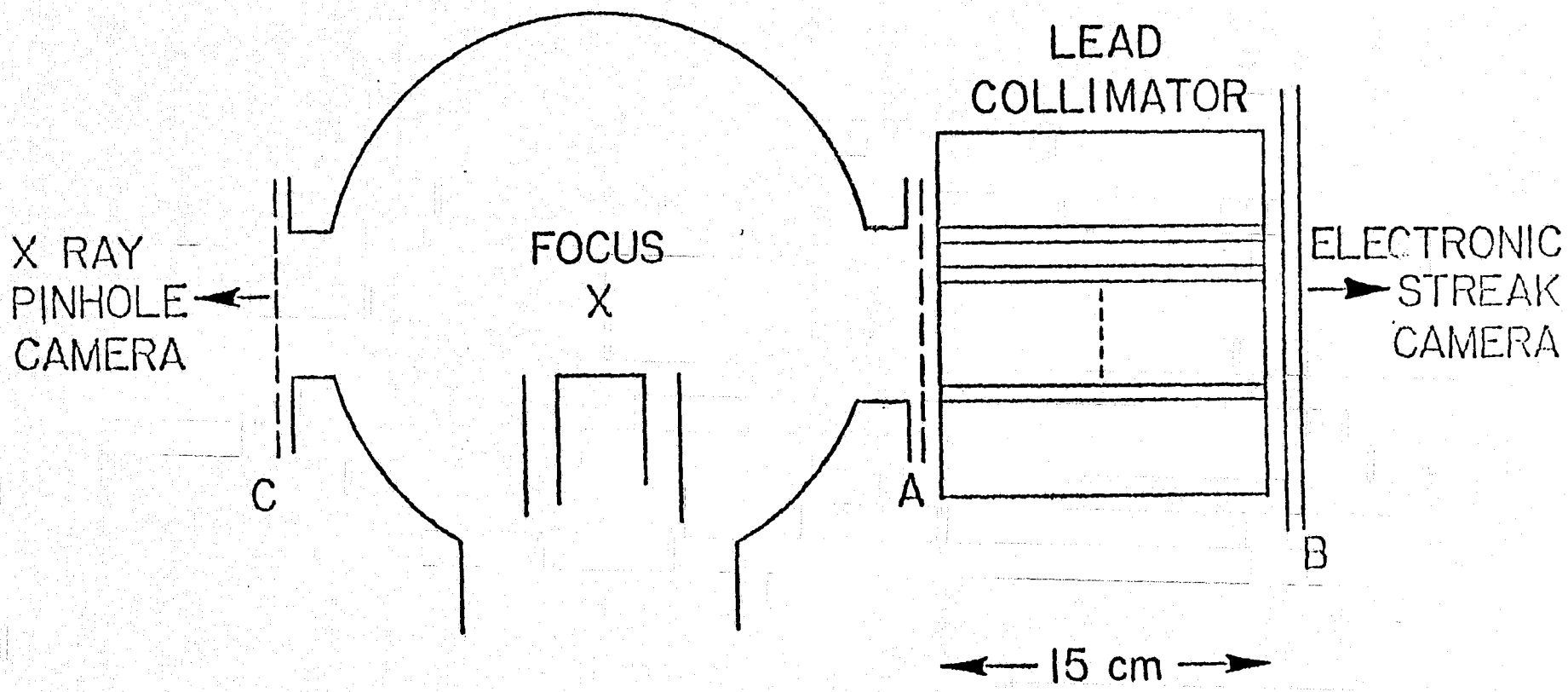

Fig. 1. Method of taking streak photographs.

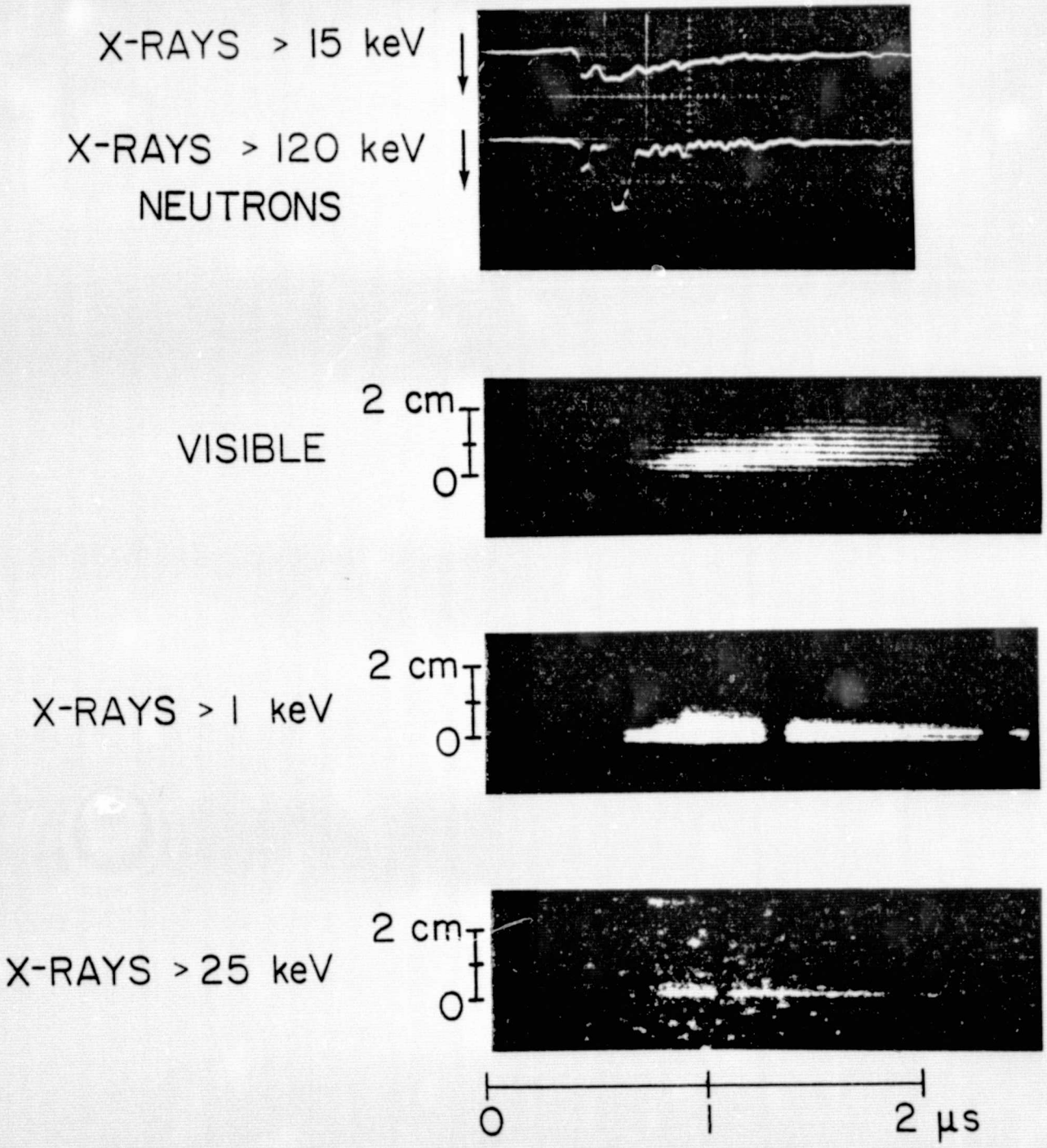

Fig. 2. Streak photographs of visible light and x-rays.

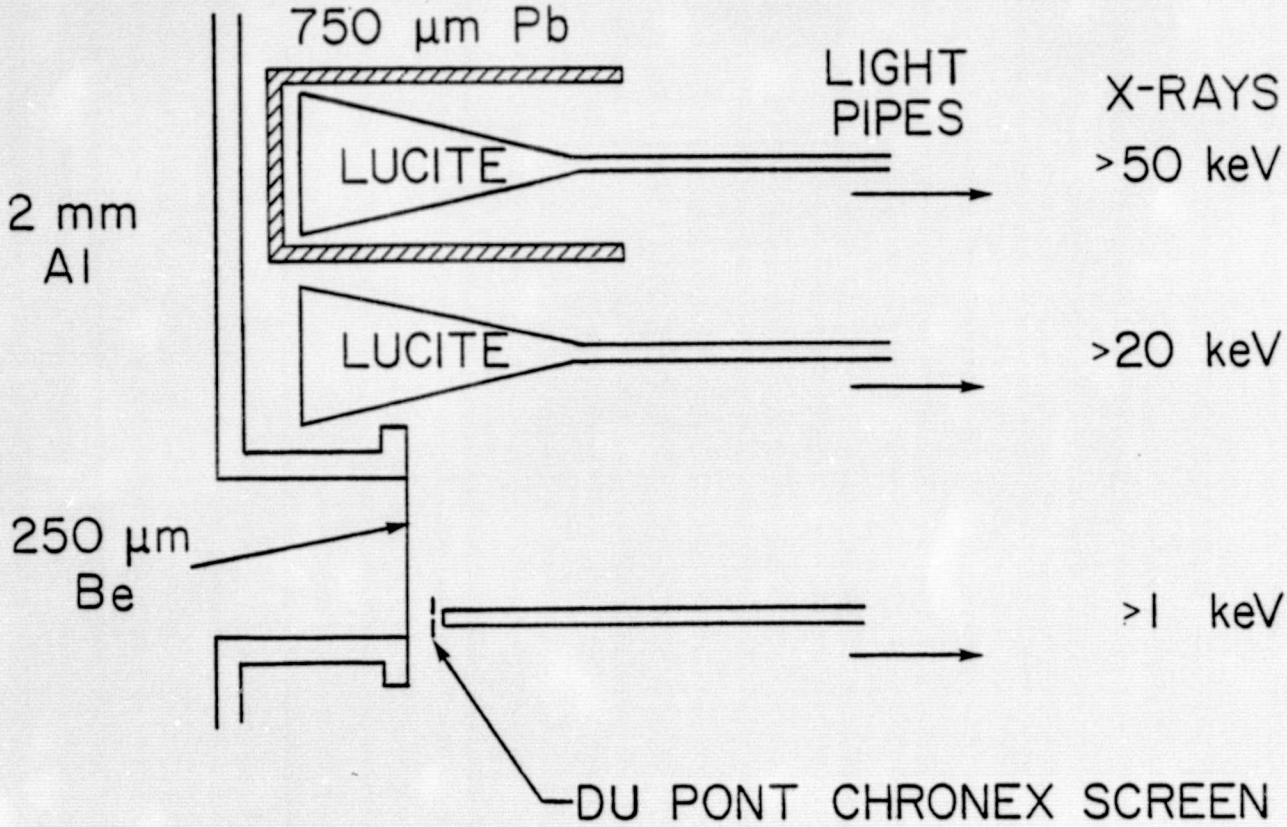

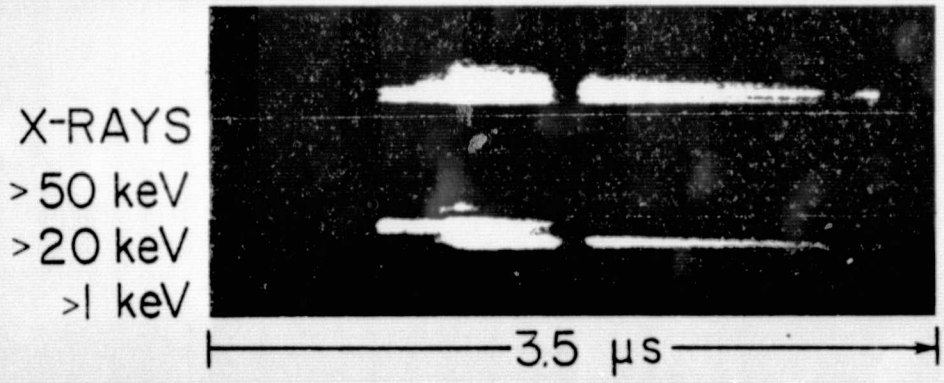

Fig. 3. Streak photographs of x-rays of different energies.

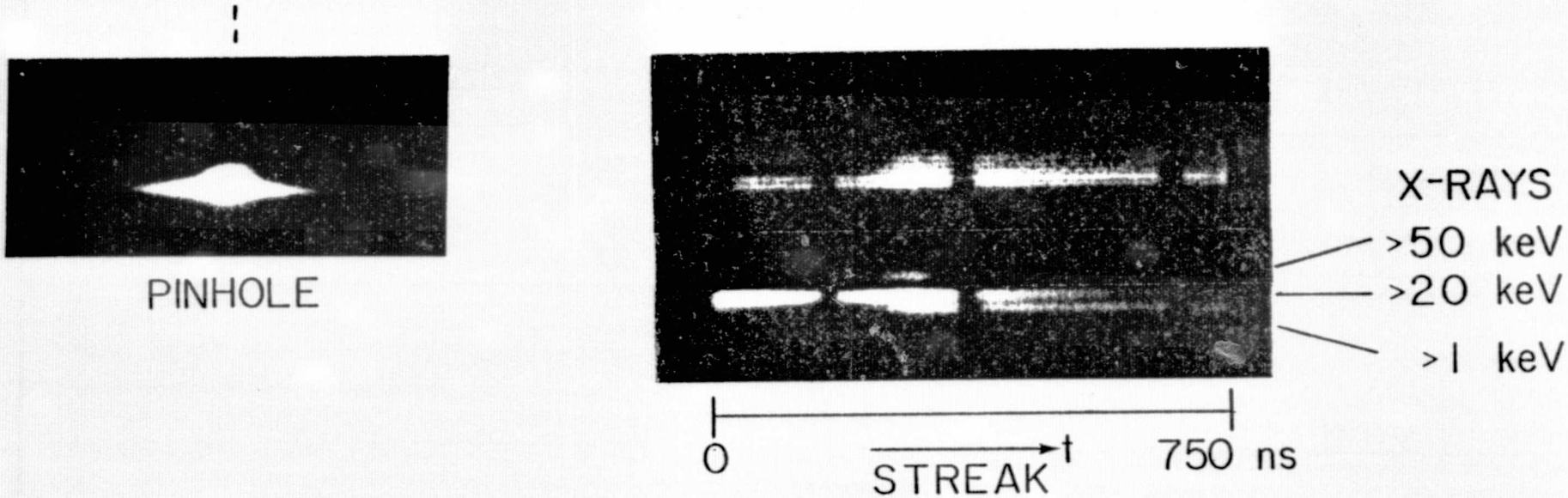

Fig. 4. Comparison of streak and pinhole photographs of x-rays > 1 keV.

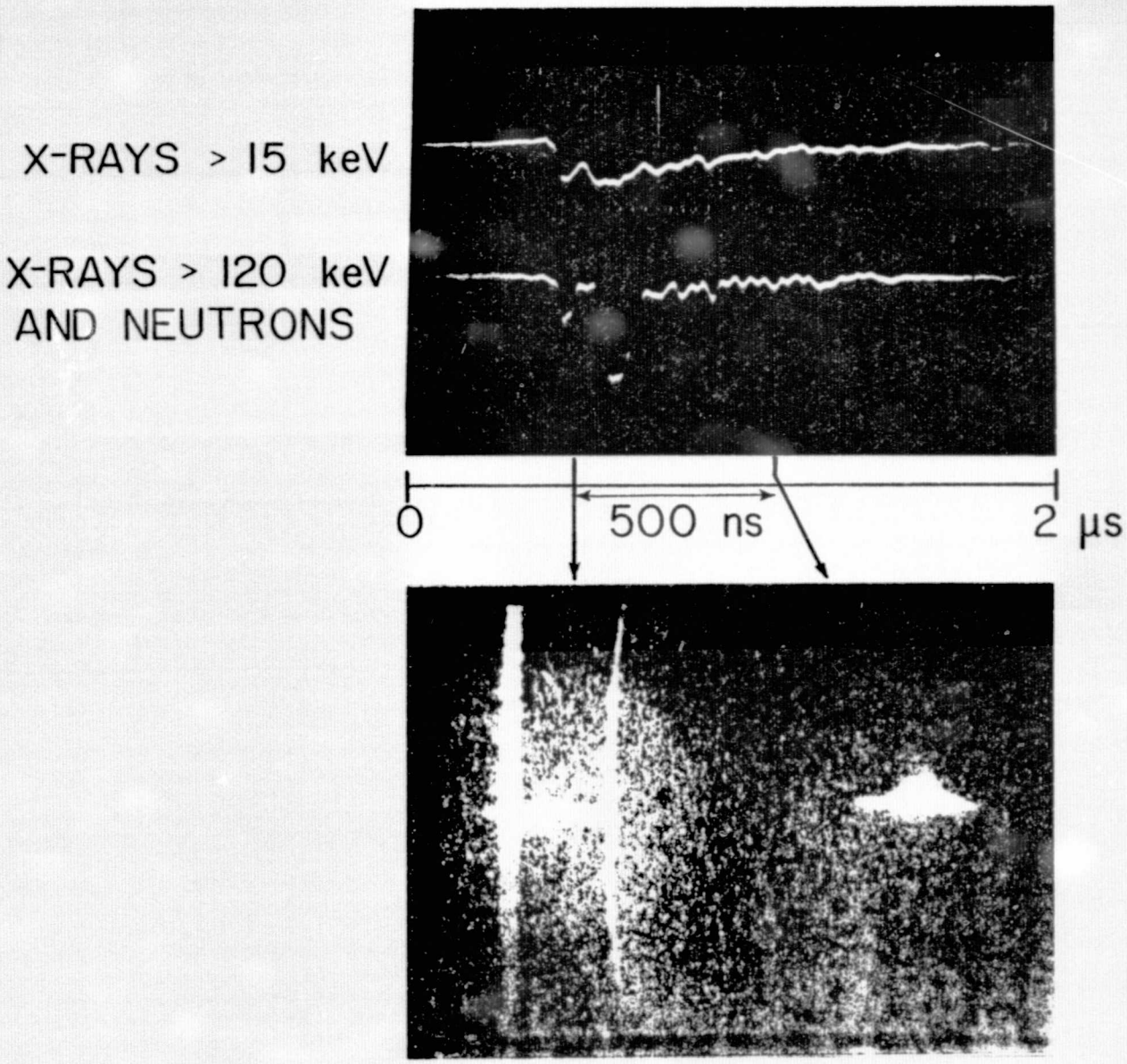

Fig. 5. Framing pictures of x-rays >1 keV.

2.1.5. Summary of the Work on Focus I

Trajectories of High Energy Electrons in a Plasma Focus

The intensity of x-rays from a plasma focus was measured versus position, time, energy, and angle of emission. The low energy x-rays emanated from the plasma, but the high energy components came from a small region of the anode surface, on axis. Emission from the focus occurred some 20 ns prior to that from the anode, but the latter continued for 500 ns. X-ray "shadow" techniques showed that the high energy electrons traveled in a beam almost perpendicular to the anode surface. Spatial plots of x-ray intensity at different energies showed that the electrons gained energy as they approached the anode. No counter streaming of high energy electrons away from the anode was evident. Polar diagrams of medium-energy ($\approx$ 20 KeV) x-rays resembled a cardioid, but high energy ($\approx$ 100 KeV) x-rays were emitted in a narrow lobe toward the anode, with a forward-to-back ratio of about 50; both results were consistant with bremsstrahlung emission from a beam of relativistic electrons. The relativistic beam current was estimated at several 100 A. The electric fields required to produce such electron trajectories are also consistant with the observed anisotropy of ion emission in a focus, and with the converging beam model of neutron production, proposed previously.

Space and Time Resolved Emission of X-Rays from a Plasma Focus

The x-ray emission from the on-axis region of a plasma focus was observed through a lead collimator (spatial resolution $\approx$ 1 mm), and recorded on an image intensifier screen. An electronic streak camera combined with an image intensifier (system gain up to 500,000) gave time resolution of about 10 ns. Although x-rays from the focus could not be detected, x-rays (>1 KeV) appeared thereafter near the anode surface, and the edge of the emission region moved away at roughly 10^4 ms^{-1} until it was 2 cm away. Framing pictures of the pinhole image on the screen confirmed these results. Hard x-rays (>20 KeV) behaved similarly but were detected only to about 1 cm from the surface. The x-rays were from copper vapor released by a beam of electrons on axis, and emission occurred where both the beam energy and the copper density were high. The recorded emission from the focus region occurred

hundreds of nanoseconds after the focus was over. This suggests that magnetic flux annihilation continued for this duration to sustain the electric field driving the electron beam.

2.2. The Staged Plasma Focus

The staged plasma focus was conceived by Dr. J. H. Lee (ref. 5), and the work reported in this section was done in collaboration with him and D. R. McFarland. The device has been in operation since August 1976. A general description is given in section 2.2.1 followed by the results of the experiments in the next two sections. The results are summarized in section 2.2.4.

2.2.1. A Staged Plasma Focus--General Discussion

The dense plasma focus (ref. 1) and the noncylindrical Z-pinch (ref. 2) apparatus have demonstrated that copious nuclear fusions can take place in plasmas at near fusion reactor conditions. However, previous attempts to couple two plasma focuses have been unsuccessful for both types of apparatus (refs. 3, 4). Hence, the development of a large-scale reactor by combining a number of such devices has hitherto not seemed feasible.

The cross sections of the two types of plasma focus, namely (a) the Mather geometry, and (b) the noncylindrical Z-pinch or Fillippov geometry are shown in figure 1. These devices are widely used and have been energized with up to 1 MJ capacitor banks, and attained 10^{12} nuclear fusions per pulse in deuterium. The center line in the figure indicates the axis of the rotational symmetry of the devices. The letters C and SW stand for the capacitor bank and the current switches, respectively. Earlier attempts of combining two plasma focuses (fig. 1(c) and (d)) showed a current sheet was formed in only one of the two guns, as indicated by the dotted curves, even though both guns were fired simultaneously. Thus, simultaneous formation of two plasma foci in the combined devices has never been observed.

Two new geometries, a hypocycloidal pinch and a staged plasma focus were conceived by J. H. Lee to overcome the above difficulties (fig. 2). The hypocycloidal pinch apparatus consists of three disk electrodes with a hole in their centers. The production of a pair of plasma foci and their subsequent interaction in the center hole has been confirmed by observation with fast photography, x-ray pinhole photography and neutron detection.

The radial stability lasting 5 μs, and near complete absorption of CO_2 laser energy, have been reported elsewhere (ref. 5).

The staged plasma focus consists of a pair of coaxial guns coupled muzzle to muzzle with a conducting disk placed between the outer electrodes (fig. 2(a)). This geometry superficially resembles the two-gun combination shown in figure 1, but, as will be shown, the current sheet dynamics in the final collapse phase is very different.

Mather had suggested in 1965 that the precursor radiation produced a predischarge in the opposite gun which interfered with the final plasma collapse (ref. 3). In the staged plasma focus, as well as in a hypocycloidal pinch, the disk placed in the midplane prevents any interaction of precursor radiations with the current sheets in the opposite gun both during their formation and the run-down phase. In addition, the midplane disk in the staged focus together with the ends of the center electrodes provides a hypocycloidal-pinch geometry where the current sheets collapse toward the axis to give a pair of plasma foci. Note the center lines when comparing the two geometries. The dotted curves indicate the current sheets, which are shown three dimensionally in figure 3.

The simultaneous production of a pair of plasma foci is realized by the self-stabilizing mechanism of the hypocycloidal-pinch geometry, presented elsewhere (ref. 5). Thus, the staged plasma focus may be considered as an alternate embodiment of the hypocycloidal pinch and is, therefore, fundamentally different from the two open-ended gun assemblies.

The advantages claimed for the hypocycloidal pinch are also applicable to the staged plasma focus: (1) large plasma volume, (2) longer stability, (3) easy access for additional heating, and (4) a possibility of constructing a multiple array for high-power operation.

Further advantages of the staged plasma focus compared with the hypocycloidal pinch are: (1) The impedence of the guns can be matched easily with a given energy storage system by altering of the length of the cylindrical electrodes (the hypocycloidal pinch apparatus necessitates an extremely fast power system due to its fixed low inductance). Impedance matching is important for maximizing the efficiency of the system, the momentum of the

current sheets, and for proper timing of the current sheet collapse. (2) Uniform breakdown over the insulator between the electrodes can be easily realized as the insulator in the staged plasma focus is relatively small compared with that of the hypocycloidal pinch.

A further advantage of the staged plasma focus and the hypocycloidal pinch geometry is that a quiescent plasma at near nuclear fusion conditions ($T_i \approx 1$ KeV, $n_i \approx 10^{19}$ cm^{-3}) is produced by the interaction of a pair of the plasma foci. The confinement geometry of the plasma is similar to the Cusp mirror machine except that the role of the current and the magnetic field are interchanged. The magnetic configuration is a minimum B type geometry (fig. 3), and therefore should be stable. The plasma could be further heated or compressed by other schemes, such as magnetic compression, linear implosion (ref. 6), electron or ion beam heating.

The prototype staged plasma focus was constructed and details are given in section 2.2.2. Its operation was the same as for the dense plasma focus. Besides the routine monitoring of electromagnetic signals, the diagnostics employed were (1) fast image converter photography in both streak and framing modes, (2) x-ray pinhole photography, (3) x-ray and neutron flux detectors, and (4) neutron fluence measurement with a calibrated silver activation counter.

The purpose of the experiments was to (a) examine the behavior of the current sheet formation and (b) to establish whether the two foci formed simultaneously and independently.

Item (a) is dealt with in more detail in section 2.2.2 and item (b) in section 2.2.3.

References

1. J. H. Lee, L. P. Shomo, M. D. Williams, and H. Hermansdorfer, Phys. Fluids 14, 2217 (1971).

2. V. S. Imshennik, N. V. Filippov, and T. I. Filippova, Nuclear Fusion, 13, 929 (1973).

3. J. W. Mather, Phys. Fluids 8, 366 (1965).

4. A. M. Andrianov, et al., Second U. N. Int. Conf. on the Peaceful Uses of Atomic Energy 31, (1958).

5. J. H. Lee, D. R. McFarland, and F. Hohl, Phys. Fluids 20, 313 (1977).

6. S. G. Alikhanov, V. P. Bakhtin, V. M. Brusnikin, I. S. Glushkov, A. D. Muzychenko, V. P. Novikov, E19-2, Sixth International Conf. on Plasma Physics and Controlled Nuclear Fusion Research, IAEA-CN-35, 1976.

List of Figures

Figure 1. Dense plasma focus and noncylindrical Z-pinch.

Figure 2. Staged plasma focus and hypocycloidal pinch.

Figure 3. Cutaway views of the staged plasma-focus apparatus and the hypocycloidal pinch.

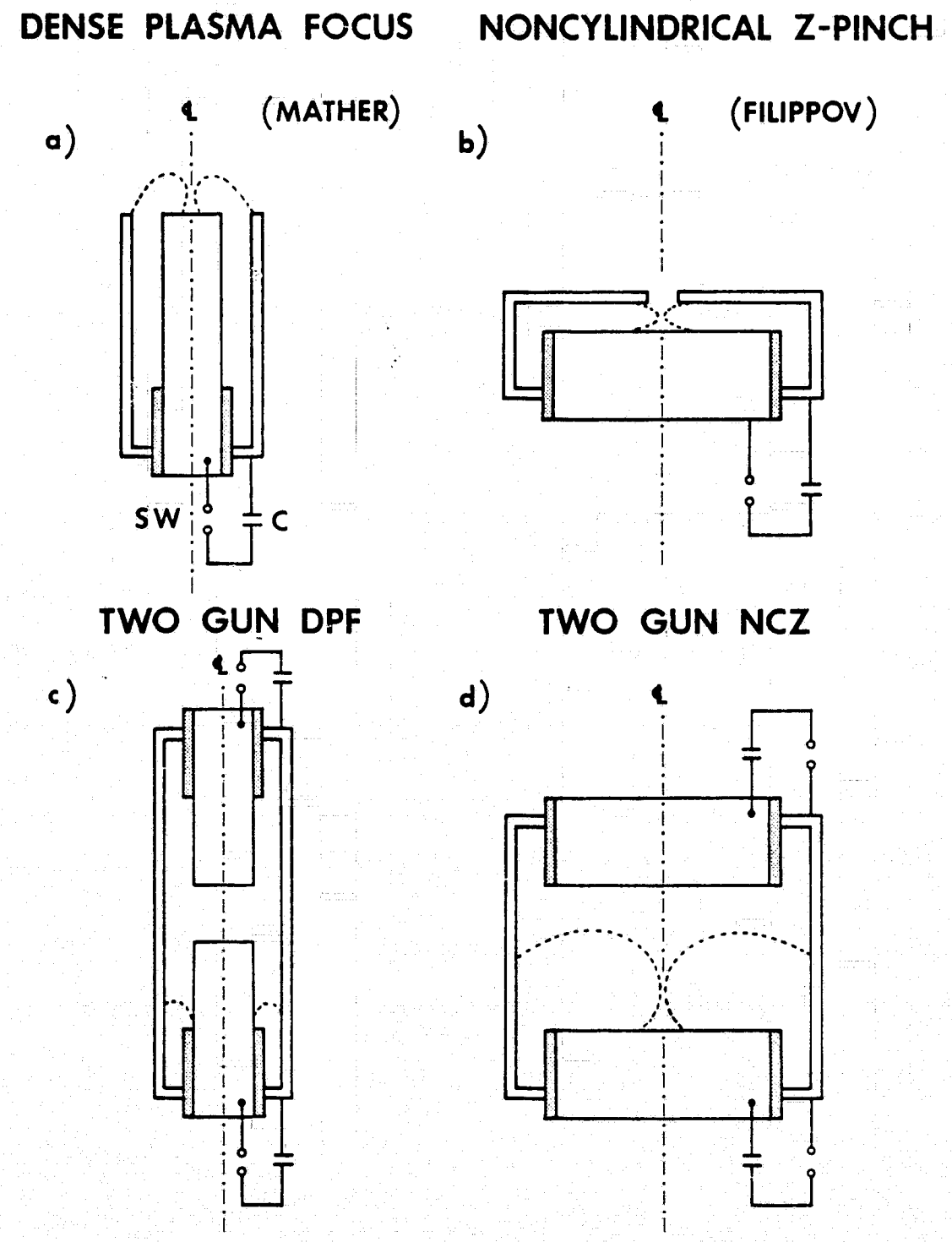

Fig. 1. Dense Plasma Focus and Noncylindrical Z-Pinch.

STAGED PLASMA FOCUS HYPOCYCLOIDAL PINCH

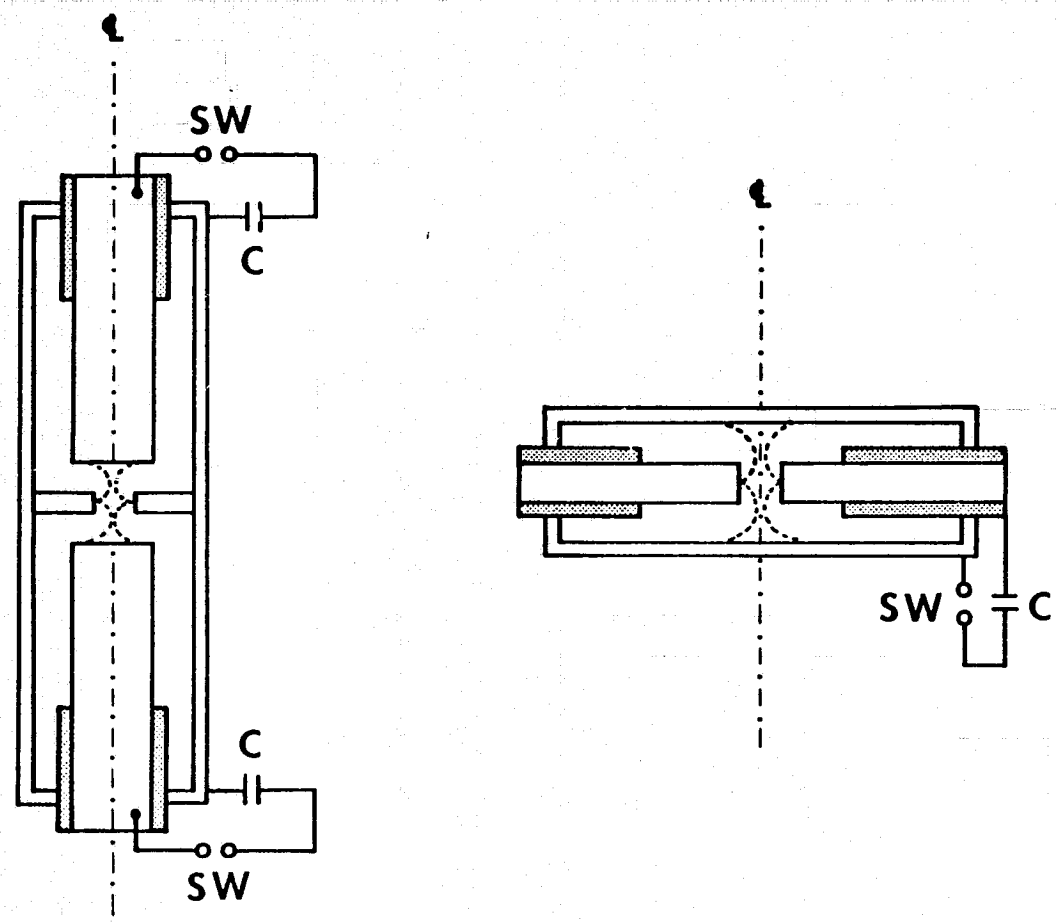

Fig. 2. Staged plasma focus and hypocycloidal pinch.

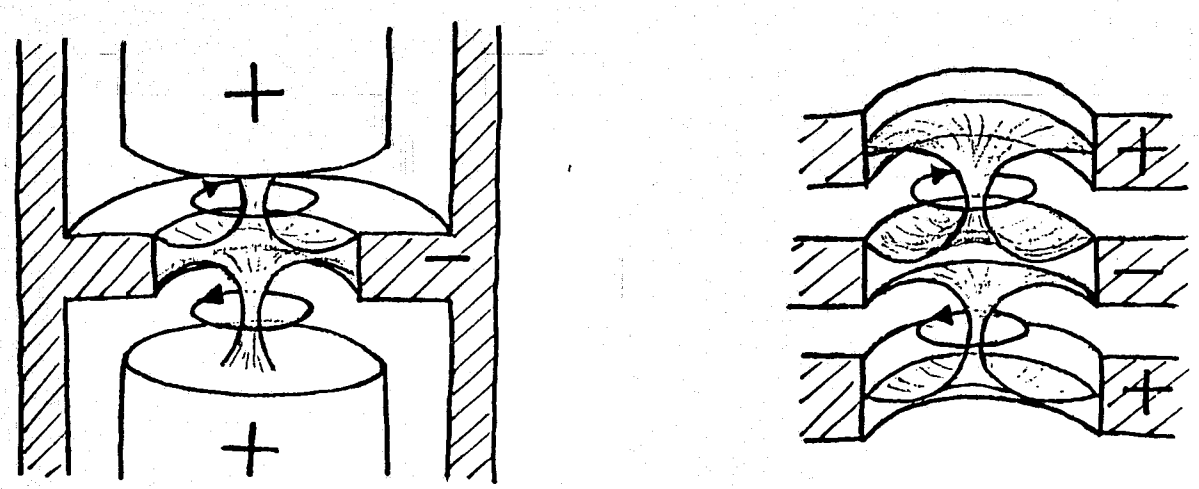

STAGED PLASMA FOCUS

HYPOCYCLOIDAL PINCH

Fig. 3. Cutaway views of the staged plasma-focus apparatus and the hypocycloidal pinch.

2.2.2. Formation of Current Sheets in a Staged Plasma Focus

Introduction

The purpose of these experiments was to investigate the formation and behavior of the current sheets in the staged plasma focus, especially to see if the two guns fired simultaneously. The parameters that were varied were type of gas, neutral gas pressure, and the polarity of the electrodes.

Apparatus

Figure 1 shows a diagram of the apparatus. The two guns were similar and consisted of an inner electrode 5 cm in diameter surrounded by an outer electrode of 10 cm in diameter and 23 cm long, which extended 2.3 cm beyond the inner electrode. The outer electrode was a cage of copper wires 2 mm in diameter and 8 mm apart. The wires were connected together by two rings midway and at the ends. The cage structure was used to reduce mass loading on the current sheets, and also to provide viewing accessibility. The vacuum vessel consisted of transparent plexiglass.

The metallic disk inserted at the midplane was 2.5 cm thick. The disk shielded the annular spaces between the electrodes of the guns from each other, as the hole in the disk had a smaller diameter than the inner electrode. Therefore, radiation from one sheet was prevented from interacting with the other.

The jitter in the breakdown of the two guns was avoided by using a common trigatron switch. The switch consisted of a pair of electrodes separated by air at an initial pressure of two atmospheres. Switching was achieved by reducing the pressure to one atmosphere, as the breakdown voltage followed the high pressure branch of a Paschen curve. Each gun was connected to the switch with 12 cables, which ensured simultaneous breakdown.

The capacitor bank used was 17 kJ at 20 kV, and the inner electrodes could be made either positive or negative.

The gases used were deuterium at pressures ranging from 0.1 to 20 torr and helium from 1 to 16 torr.

Diagnostics

The main diagnostics used in these experiments were an image converter camera used in the streak and framing modes, and a number of collimators observing visible light from the plasma. The collimators enabled the arrival times of the current sheets at various points to be determined. Several narrow pipes at the midplane observed a region approximately 0.5 cm diameter and two wider pipes on either side observed the individual sheets. The latter, which had variable aperture, could observe an area approximately 2 cm diameter sufficient to cover the focus even if it were misplaced from the axis. Light pipes led from the collimators to photomultipliers.

Results

Figure 2 shows a streak photograph of the current sheets. This shot is for deuterium at 4 torr with the center electrodes negative. The streak duration was 6 μs, and the luminous fronts were recorded for 5 μs. The arrival of the sheets at midplane was detected by a midplane collimator and shown on the upper trace of the lower photograph. The field of view of the camera included the region AB, and the two rings (used as distance marks) and the disk are evident. It can be seen that the two sheets arrived at A and B simultaneously and proceeded with equal and opposite constant velocities. Although the disk obscures the midregion, the focus is shown by a halo from overexposure at the point in time just after the two sheets reached the ends of the electrodes. The streak of light below is from a collimator in the disk. The velocity of the sheets is 3.6×10^4 ms^{-1}. A rough estimate can also be made of the velocities with which the interacting plasmas approached each other, and turns out to be about 3×10^4 ms^{-1}.

An example of a framing picture of the two sheets taken at a neutral pressure of 0.6 torr of deuterium with the center electrode negative is shown in figure 3. The exposures were 20 ns taken 500 ns apart. The luminous sheets appear to be about 2 cm thick, and have equal and opposite constant velocities of 7×10^4 ms^{-1}.

The velocities of the current sheets were obtained from both streak and framing pictures taken at different gas pressures for deuterium and helium.

Figure 4 shows sheet velocity V versus filling pressure p for deuterium, with the center electrode positive. The dependence follows.

$$V \propto p^{-n} \; ; \quad n = 0.25 \pm 0.05$$

for the range $0.5 < p < 6$ torr. The results were similar when the center electrode was negative, and in the same pressure range the velocities were roughly the same. The straight line on figure 4 shows a slope of -0.25. For pressures below 0.5 torr the velocities tended to become independent of p and at pressures greater than 6 torr were below the straight line. Measurements on helium for $1.5 < p < 10$ torr showed the sheets behaved similarly to those in deuterium.

Recently Karpov, Smirnov and Suvorov (ref. 1) published a theoretical treatment of the axial motion of a current shell in a dense plasma focus, and showed that after a brief period of acceleration, the velocity of the current sheets should be constant, and the velocity should obey

$$V \propto [\rho_0(\gamma + 1)]^{-0.25}$$

where ρ_0 is the density of the unperturbed gas and γ the ratio of specific heats. Thus out experimental results agree in the dependence on ρ_0 or p the filling gas pressure. The theory predicts that the velocities in helium should be a few percent lower than those in deuterium because of the difference in γ, whereas ours were about 20 percent higher. We are unable to explain this discrepancy.

A rough measure of the similarity in behavior of the two guns could be obtained by comparing the visible light signals from the two focus regions.

Light signals from two collimators observing areas 2 cm square are shown in figure 5. The duration of the light signals was over 10 μs but the sheets from both guns arrived almost simultaneously. The instant of focus formation was obtained from a recording of x-ray emission versus time on another oscilloscope. Light emission was recorded 100 ns prior to the focus as the sheets collapsed. The overall shape of the signals implies that the

two guns behaved more or less similarly, although considerable shot to shot variations were evident. Focus formation and the emission of x-rays and neutrons from the two focused plasmas will be discussed in section 2.2.3.

Conclusions

In conclusion we have found that it is possible to operate the two guns of a staged focus with sufficient simultaneity that the two focuses occur within the same time span. The current sheets were formed independantly, and the luminous regions were a few cm thick. Their velocities were from 2.5 to 8×10^4 ms^{-1} and depended on pressure as expected from theory. The successful formation of simultaneous current sheets in the two guns opens the possibility for developing a higher powered device by utilizing the interaction of focused plasmas.

Reference

1. G. V. Karpov, E. N. Smirnov, and V. N. Suvorov, Sov. Phys. Tech. Phys. 21, 293 (1976).

List of Figures

Figure 1. Diagram of apparatus.

Figure 2. Streak camera picture of current sheets.

Figure 3. Framing pictures of current sheets.

Figure 4. Velocity of current sheets versus neutral pressure of deuterium.

Figure 5. Light pipe signals.

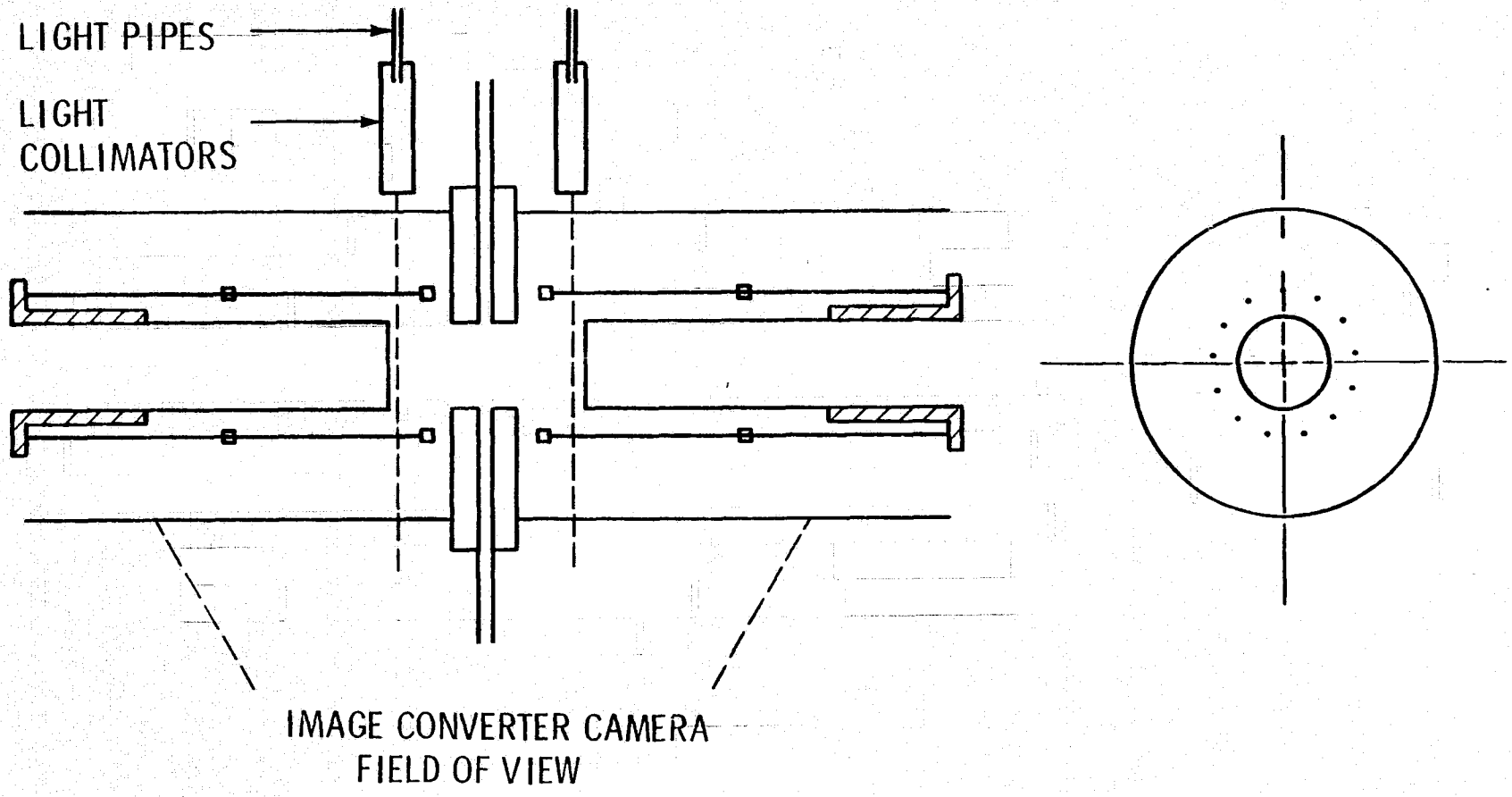

Fig. 1. Diagram of Apparatus.

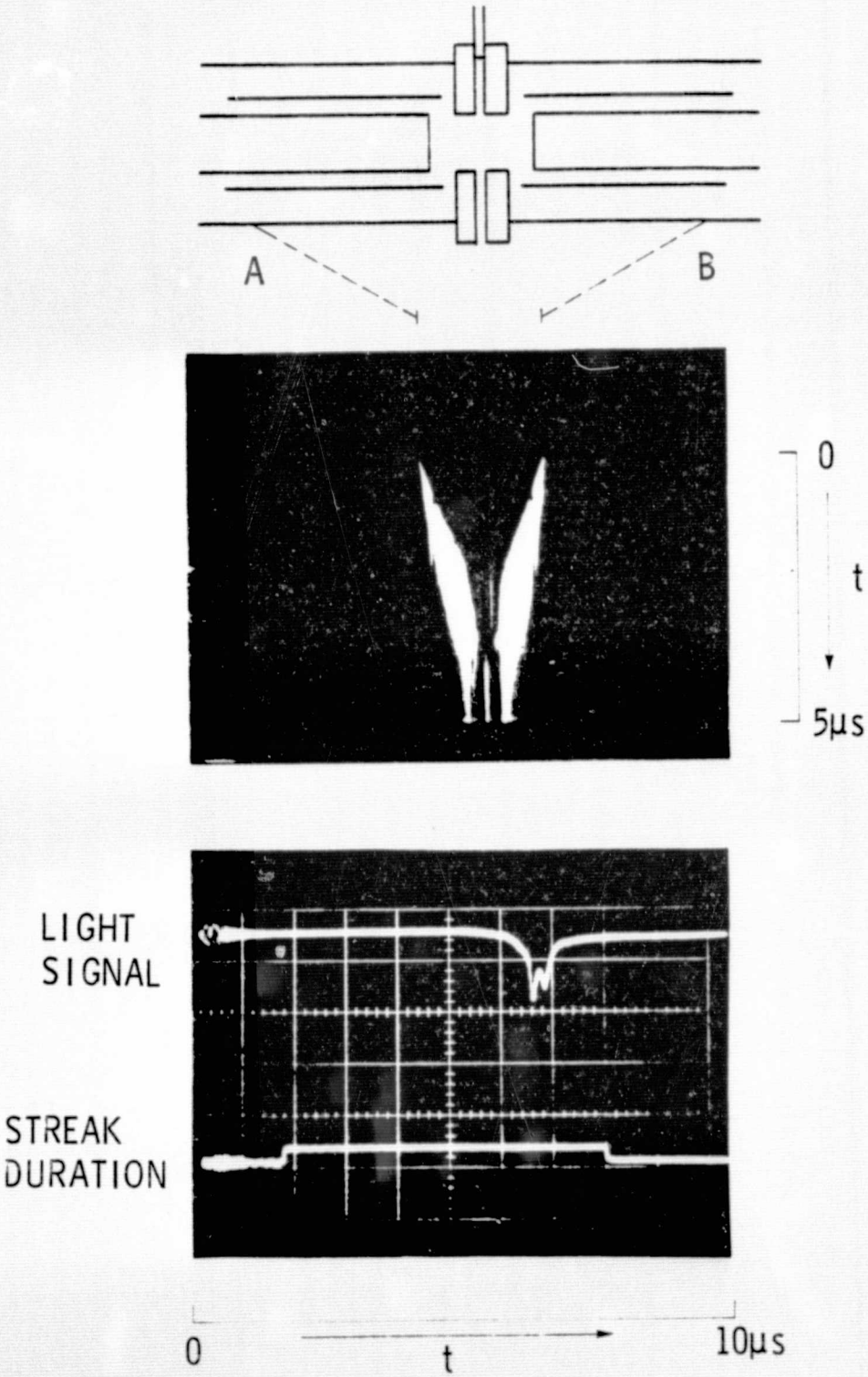

Fig. 2. Streak camera picture of current sheets.

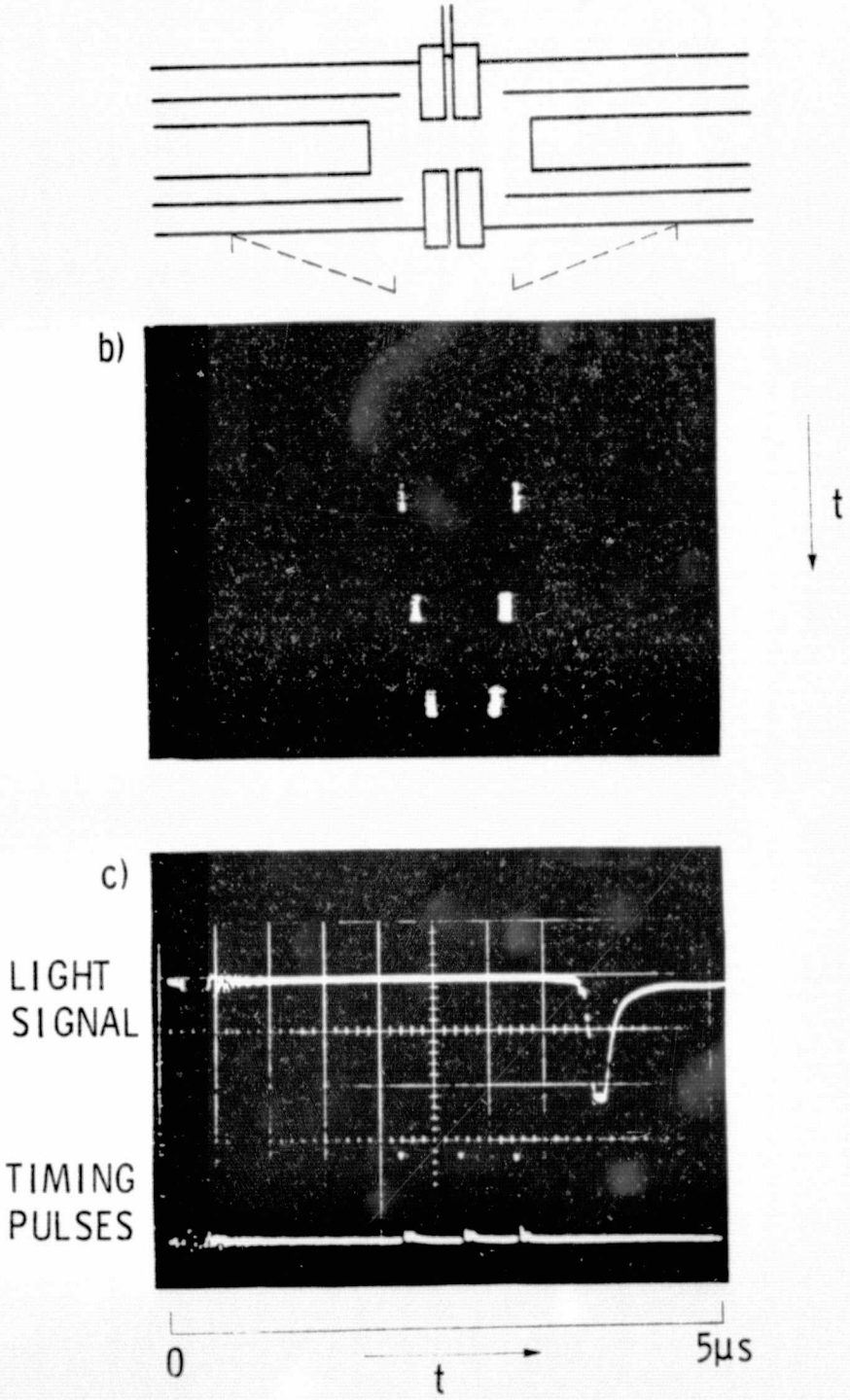

Fig. 3. Framing pictures of current sheets.

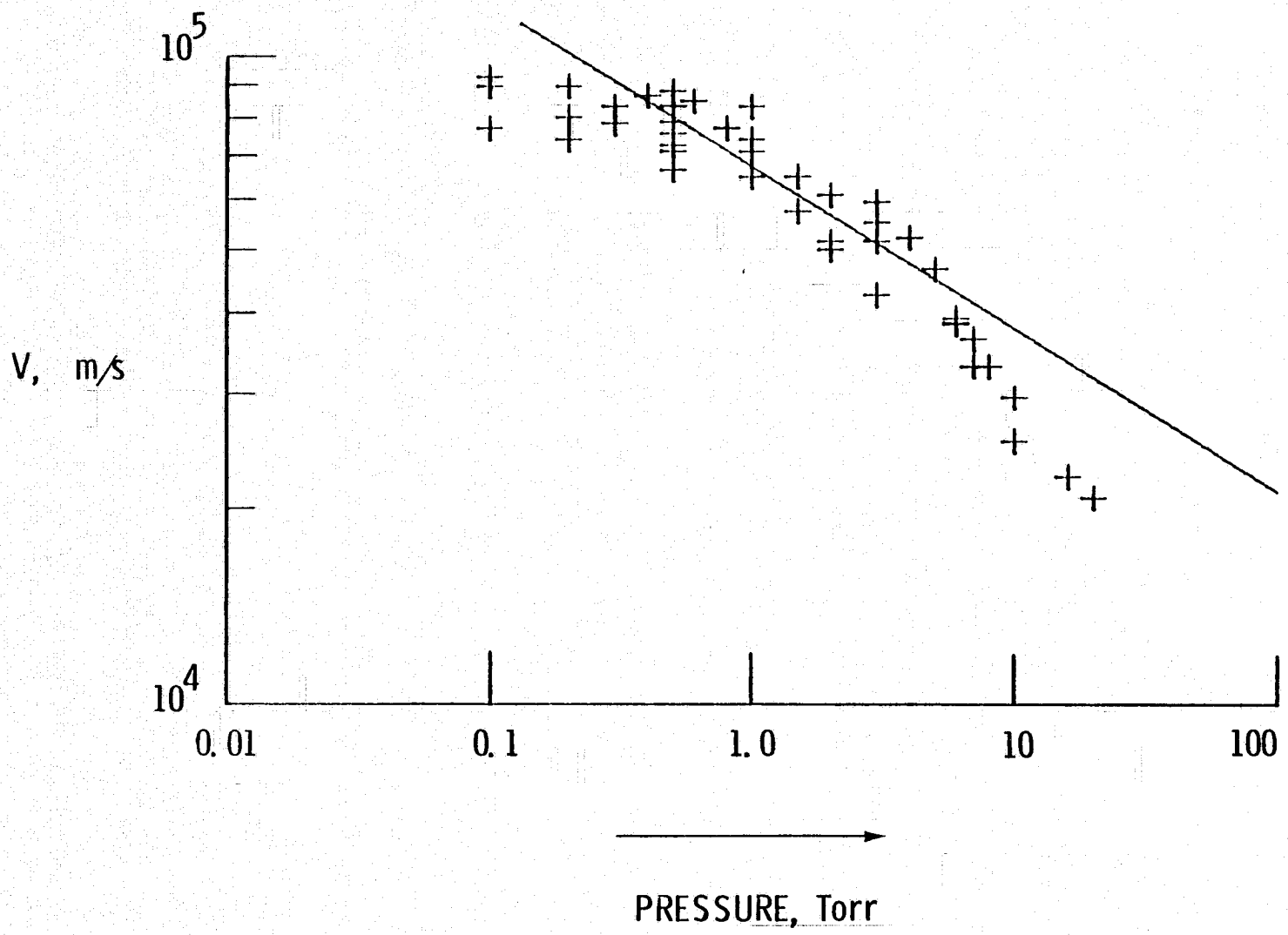

Fig. 4. Velocity of current sheets vs neutral pressure of deuterium.

a)

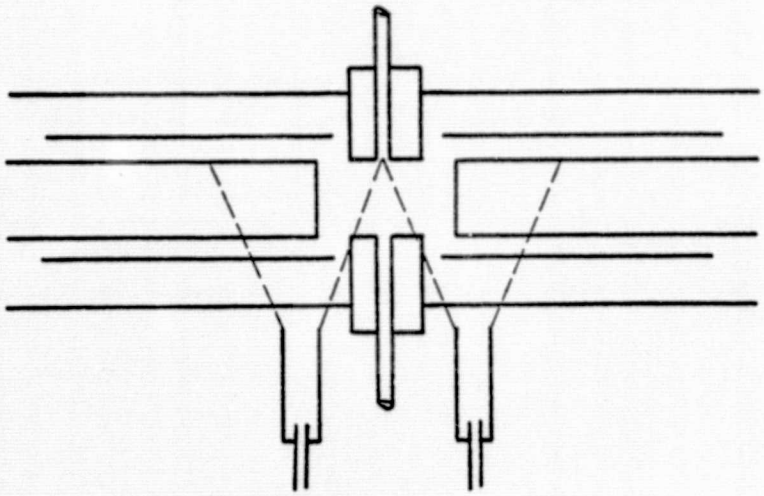

b)

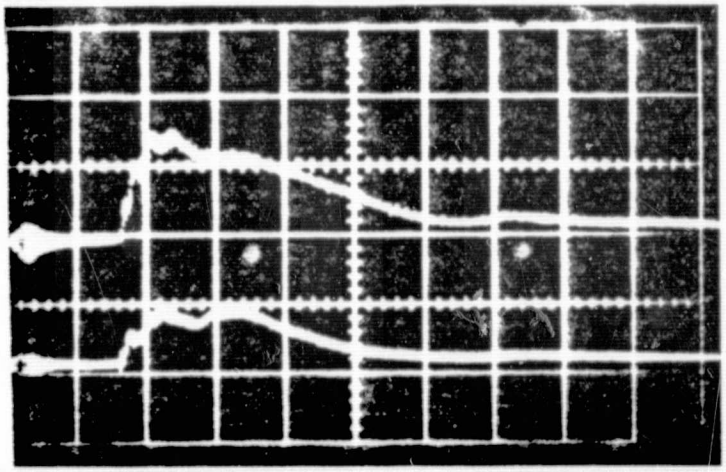

0 → 20μs

t

Fig. 5. Light pipe signals.

2.2.3. X-Ray and Neutron Emission from a Staged Plasma Focus

Introduction

The purpose of these experiments was to investigate the x-ray and neutron emission from the staged plasma focus and in particular to see if the two guns operated simultaneously. Both time and space resolution were obtained. The central electrodes were positive for these experiments.

Experimental Results

We first recorded the hard x-ray and neutron emission as functions of time by using NE102 scintillators observed by photomultipliers. Two such detectors were used, one 3 m from the apparatus, and the other 8 m away; thus time of flight separation of the x-rays and neutrons was possible. Each of the detectors recorded the emission from both guns, and two separate runs are shown in figure 1. Separation of the x-ray and neutron signals due to their time-of-flight difference is evident. The x-ray emission occurs over a period of 100 ns as can be seen from both detectors. The neutrons are clearly separated from the x-rays and took about 160 ns and 360 ns respectively to arrive at the two detectors. The emission time of the neutrons is also of the order of 100 ns. We note that the x-ray and neutron signals consist of a single peak for the upper picture. Most of the time the behavior recorded was as shown here although on some occasions x-ray and neutron signals with double peaks were seen on both detectors as shown in the lower picture. For the majority of shots with single peaks the two guns must have formed focuses simultaneously, or else only one gun formed a focus. Therefore further experiments were performed to provide spatial resolution between the two guns.

Figure 2 shows an experiment which proves that x-rays were emitted from both guns simultaneously. A 5 cm thick block of lead was placed as shown so that the 3 m detector could only observe the right gun, and the 8 m detector only the left. Preliminary experiments had shown that the lead could cut off the x-ray signals, but not necessarily the neutrons. Therefore we shall be concerned here only with the x-ray signals. Two shots are recorded.

The first shot on the first and third trace gave little x-ray emission from either gun, but adequate neutrons. The second shot gave strong signals on both detectors indicating that x-ray emission occurred from both guns. The x-ray signals were recorded almost simultaneously on the two detectors.

Our next experiment was aimed at obtaining spatial resolution of the x-ray emission using pinhole techniques. The arrangement is shown in figure 3. Two pinhole cameras A and B observed the separate guns. The pinholes were 0.4 mm diameter, in steel, backed by lead. The plexiglass wall of the vacuum chamber was removed in this region, and the vacuum was maintained by a 250 μm beryllium window which transmitted x-rays of energies greater than about 1 KeV. "No-screen" x-ray film was used. The results shown below indicate that the x-ray emission was mostly from the surface of the electrodes, similar to the operation of the guns operating singly. Clearly x-ray emission occurred from both guns.

Another pinhole camera C included both anodes in its field of view. As it was observing through the plexiglass wall of the vacuum vessel, the pinhole was considerably larger than before, approximately 3 mm in diameter, and the resolution poor. Nevertheless, single shots made two distinct images, such as shown, indicating that x-rays were emitted from both guns. Another check was made by placing a strip of film in an envelope on the outward side of the disk structure, which showed that x-rays came from both sides. On some occasions these diagnostics showed that x-ray emission came from one or other of the guns only, but in the majority of cases emission was recorded from both guns.

Next, a collimator was constructed to provide spatial resolution for neutron detection, as shown in figure 4. A 1 cm hole was made in a block of boron-filled polyethylene, 1 m thick. The near side of the block was 1 m from the plasma, so a spatial resolution of about 2 cm was possible. The detector was similar to the ones used already and was 2 m from the focus; thus time of flight separation of x-ray and neutron signals was just possible.

The collimator was then aligned on each gun in turn, while the 8 m detector observed both guns simultaneously. The two pictures show the collimator observing the left and right guns respectively for two separate

shots, on the upper traces. The neutron signal can be separated in time, and its peak occurs 50 ns after the peak of the x-rays. The lower trace is the signal to the 8 m detector. The x-rays are recorded 50 ns later than on the 8 m detector as expected, because they had to travel an extra 6 m (20 ns), and the signal from the photomultiplier had to traverse an extra 20 feet of cable. Other shots recorded neutrons from the 8 m detector but not from the collimator suggesting only one focus had been formed. The results here prove that both guns were capable of forming focuses and emitting neutrons.

Lastly, the total neutron yield per pulse was estimated by using a silver activation analysis method. The results showed that the total yield of neutrons from the apparatus was about 10^8 per pulse. The yield from both guns was approximately equal as shown by comparing the neutron signals on the 3 m detector observing the separate guns through the collimator.

Conclusions

In conclusion we have shown that the x-rays from the staged plasma focus were emitted from each gun individually. Although the focuses sometimes occurred at different times for a fraction of the shots, for the majority the x-ray emission from the two guns occurred almost simultaneously, and within much less than 100 ns, the duration of the focuses. Neutron production also occurred simultaneously from both guns, and the total neutron yield from the apparatus was around 10^8 per shot (20 KV, 17 kJ capacitor bank).

The importance of being able to produce two plasma focuses simultaneously lies in the fact that it opens the way to studying the interaction of focused plasmas. In addition, new configurations involving more than one current sheet may now be possible.

List of Figures

Figure 1. Hard x-ray and neutron emission from the staged plasma focus time-of-flight analysis.

Figure 2. Detection of x-rays from different guns.

Figure 3. X-ray pinhole cameras.

Figure 4. Detection of neutrons from different guns.

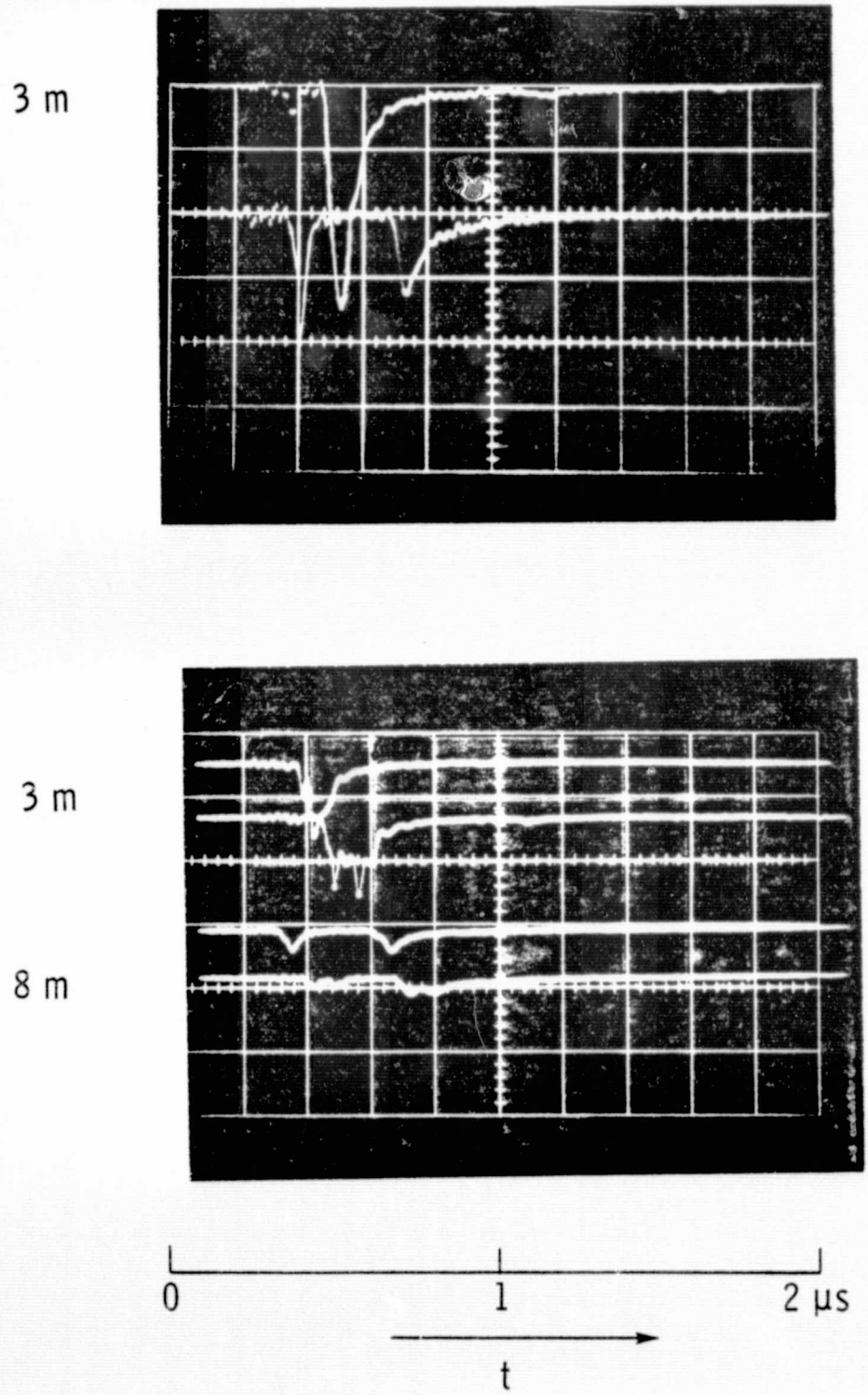

Fig. 1. Hard x-ray and neutron emission from the staged plasma focus Time-of-Flight analysis.

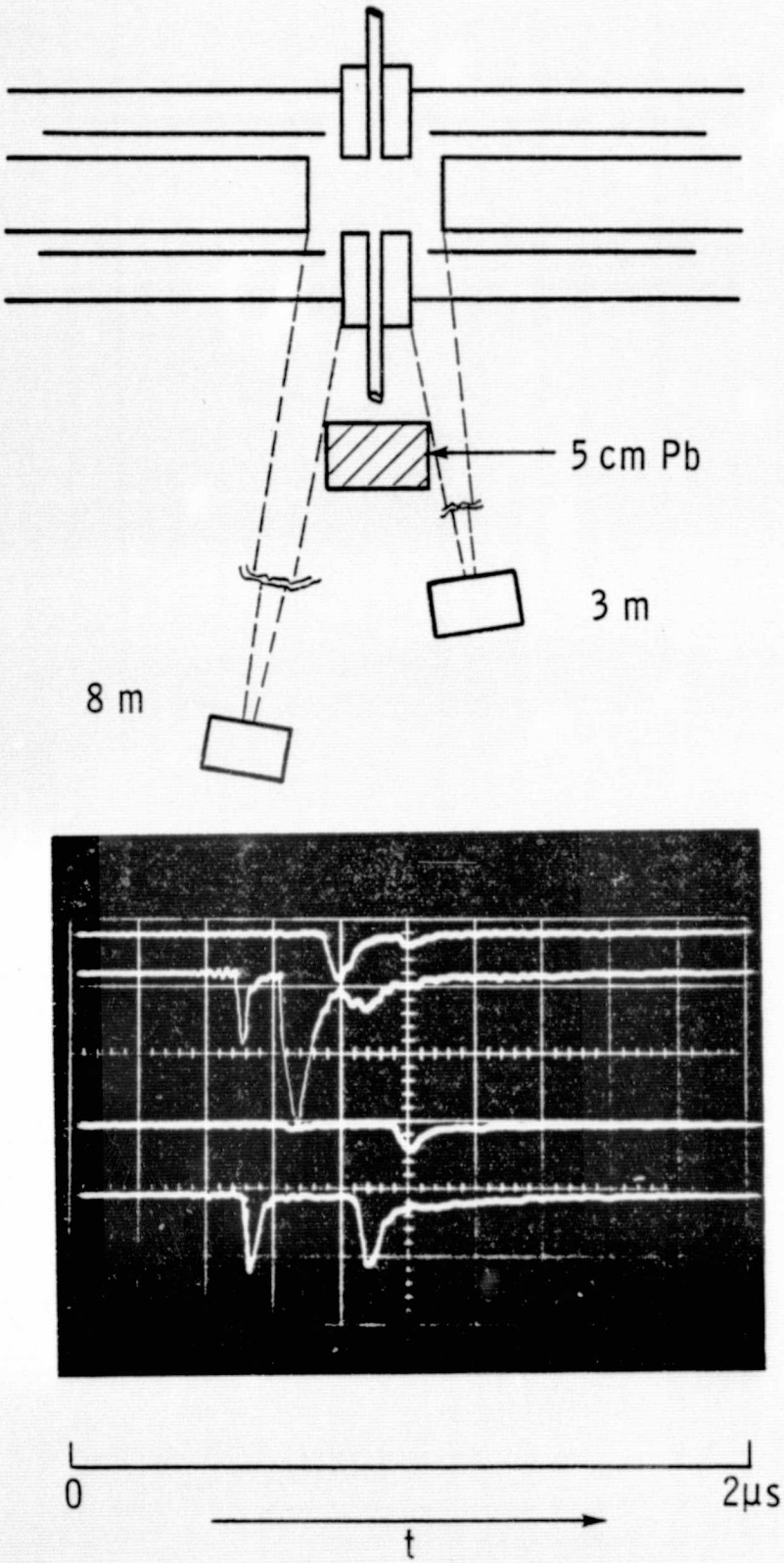

Fig. 2. Detection of x-rays from different guns.

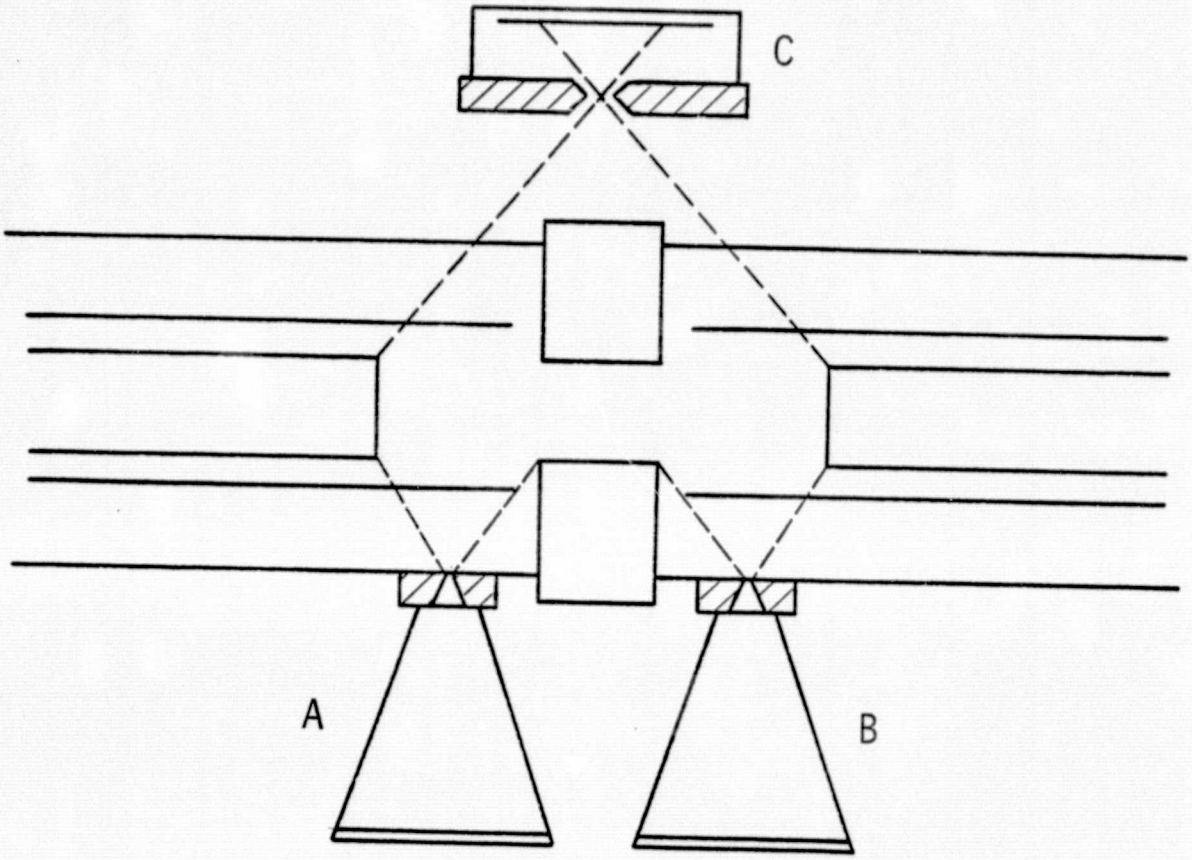

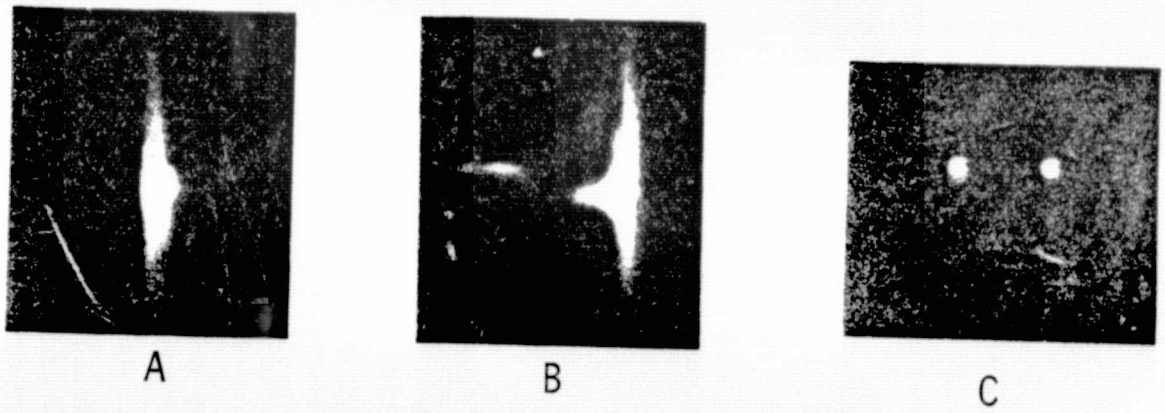

Fig. 3. X-ray pinhole cameras.

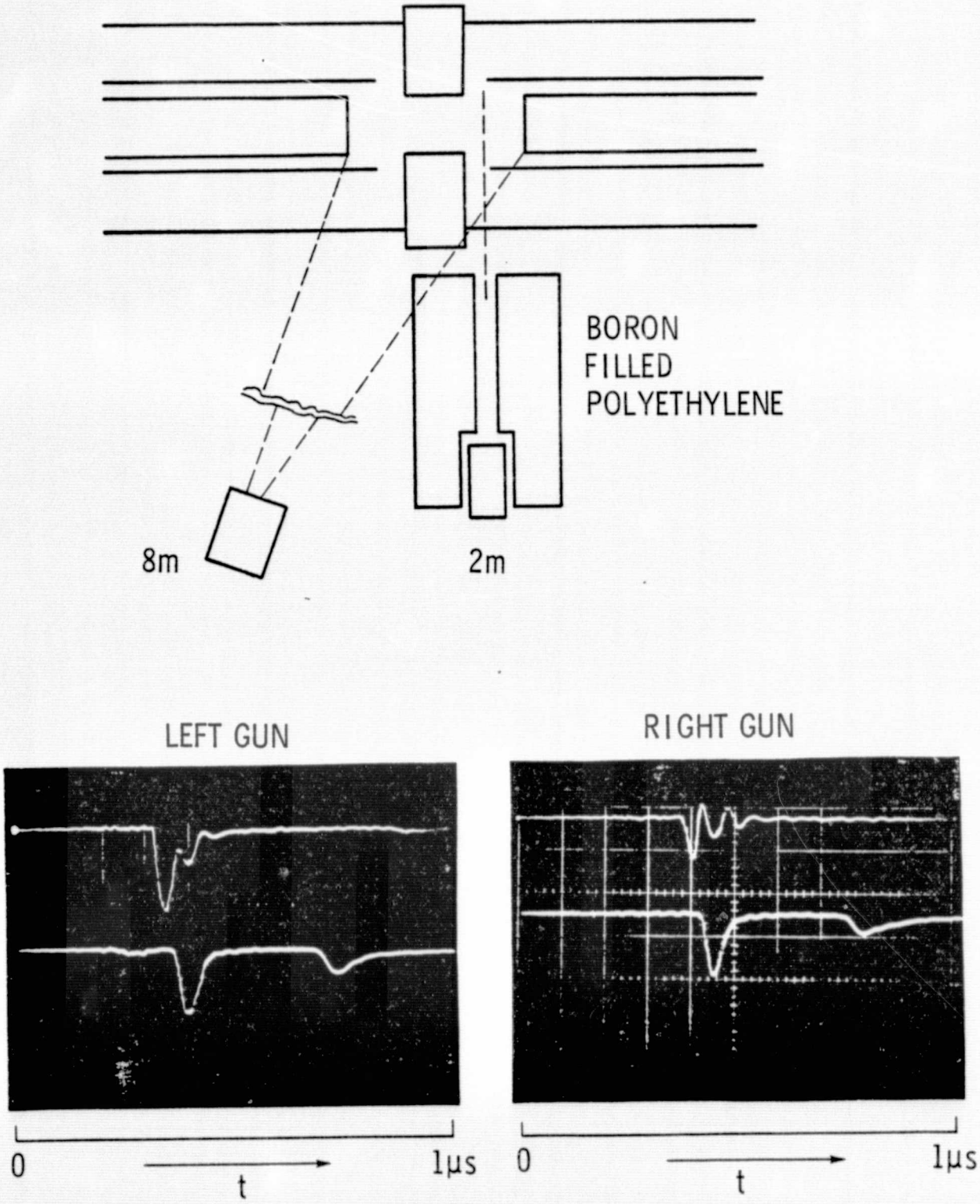

Fig. 4. Detection of neutrons from different guns.

2.2.4. Summary of Work on the Staged Plasma Focus

In brief, the results can be summarized as follows:

(1) The current sheets formed simultaneously in each of the two guns, and their run-down speeds were equal within the error of the measurement.

(2) The simultaneous formation of two plasma focuses over the center electrodes was confirmed by x-ray pinhole photographs and the pulse shape of x-ray and neutron signals.

(3) Visual inspection of the electrodes and the midplane disk after a few tens of runs also showed the erosion of the surfaces of both the center electrodes, due to bombardment of electron beams from the focused plasma and uniform polishing of the center-hole wall by particles from the plasma foci.

The significance of these results lies in the fact that it opens the possibility of operating dense plasma-focus type devices in multiple arrays at power levels beyond the scaling law for a single gun. There are already some indications that the neutron yield from the 1 MJ plasma focus (ref. 1) was reported short by an order of magnitude from the expected value. A pessimistic view has been expressed for the scaling law beyond 10 MJ based on MHD calculations (ref. 2), and engineering problems may dictate an even lower energy level.

In conclusion, a staged plasma focus as a variation of the hypocycloidal pinch was designed, and preliminary investigation was made with a prototype. The current sheet dynamics and production of a pair of plasma foci were observed as expected.

References

1. Ch. Maisonnier, J. P. Rager, C. Gourlan, P. Morgan, and M. Galanti, E18-2, Sixth International Conference on Plasma Physics and Controlled Nuclear Fusion Research, IAEA-CN-35, 1976.

2. R. A. Gerwin, Unpublished, LASL Note, 1975.

3. PUBLICATIONS

1. "Fine Structure of Hard X-ray Emission from a Plasma Focus Apparatus." W. L. Harries, J. H. Lee, and D. R. McFarland, Bull. Am. Phys. Soc., 19, 511 (1974).
2. "Space and Time Resolved Observations of X-ray Production in a Plasma Focus Apparatus." J. H. Lee, W. L. Harries, and D. R. McFarland, First IEEE International Conference on Plasma Science, Knoxville, Tennessee, 15-17 May 1974, Paper 2C11.
3. "Electron Dynamics in a Plasma Focus Based on X-ray Measurements." W. L. Harries, J. H. Lee, and D. R. McFarland, Bull. Am. Phys. Soc., 19, 945 (1974).
4. "Trajectories of High Energy Electrons in a Plasma Focus." Bull. Am. Phys. Soc., 20, 1370 (1975).
5. "Trajectories of High Energy Electrons in a Plasma Focus." W. L. Harries, J. H. Lee, and D. R. McFarland, submitted to Plasma Physics.
6. "Electron Beams in a Plasma Focus." W. L. Harries, J. H. Lee, and D. R. McFarland. Bull. Am. Phys. Soc. 22, 499 (1977).
7. "Fast X-ray Streak Photography of a Plasma Focus." W. L. Harries, J. H. Lee, and D. R. McFarland. Bull. Am. Phys. Soc. 21, 1039 (1976).
8. "Correlation of X-ray and Neutron Production from a Plasma Focus." J. H. Lee, W. L. Harries, and D. R. McFarland. Bull. Am. Phys. Soc. 21, 1039 (1976).
9. "A Staged Plasma Focus." J. H. Lee, D. R. McFarland, and W. L. Harries. IEEE International Conference on Plasma Science, May 23-25, 1977, Rensselaer Polytechnic Institute, Troy, N.Y., Paper 6C9.
10. "Formation of Current Sheets in a Staged Plasma Focus." W. L. Harries, D. R. McFarland, and J. H. Lee. ibid Paper 6C10.

11. "X-Ray and Neutron Emission from a Staged Plasma Focus." D. R. McFarland, J. H. Lee, and W. L. Harries.
ibid Paper 6C11.